DYNAMIC STABILITY OF CONICAL SHELLS BY FINITE ELEMENTS

By

SAHUS PROMSIT

Bachelor of Engineering
Chulalongkorn University
Bangkok, Thailand
1963

Master of Science
Oklahoma State University
Stillwater, Oklahoma
1965

Submitted to the Faculty of the
Graduate College of the
Oklahoma State University
in partial fulfillment of
the requirements for
the Degree of
DOCTOR OF PHILOSOPHY
May, 1970

DYNAMIC STABILITY OF CONICAL SHELLS
BY FINITE ELEMENTS

Thesis Approved:

Ahmed E. Salama
Thesis Adviser

David M. MacAlpine

Thomas Scott Dean

Donald E. Boyd

D. Durham
Dean of the Graduate College

ACKNOWLEDGMENTS

The author wishes to express his sincere appreciation to the following individuals:

To Dr. Ahmed E. Salama, who served as my major adviser, for his invaluable suggestion, interest, friendship, and guidance throughout the preparation of this thesis.

To Dr. David M. MacAlpine, who served as my graduate committee chairman, for his invaluable help.

To Drs. Donald E. Boyd and Thomas S. Dean, members of the advisory committee, for their helpful advice and encouragement.

To Dr. R. K. Munshi, Mr. Brij R. Kishore, and Mr. Eldon Hardy for their friendship.

To Mrs. Iris McPherson of the University Computer Center for her suggestion concerning the use of its library.

To my parents, for their patient understanding and financial support.

To Mrs. Carl Estes, who typed the manuscript.

Sahus Promsit

May, 1970

Stillwater, Oklahoma

TABLE OF CONTENTS

LIST OF TABLES

LIST OF FIGURES

NOMENCLATURE

$\{a_k\}$	time independent constant matrix
dA	elemental area prior to deformation
$[A^j]$	matrix used in formulating the elemental stiffness matrix
$\{b_k\}$	time independent constant matrix
$[B^j]$	matrix used in formulating the elemental stability coefficient matrix
C	$\frac{Eh}{1-\nu^2}$
$[C^j]$	elemental matrix due to external applied loads
D	$\frac{Eh^3}{12(1-\nu^2)}$
e	initial state
E	Young's modulus of elasticity
$f(t)$	unknown functions of time
$\{G_i\}$	constant matrix
h	thickness of the shell
i	number of half waves along the meridional direction of the shell
$I_{\gamma\delta}$	$\int_0^{l_p} r^{\gamma} s^{\delta} ds$
j	number of circumferential waves
k	integer
$[k]$	elemental stiffness matrix of the p^{th} element in the j^{th} harmonic

$[k^e]$	elemental stiffness matrix at the initial state
$[K]$	structural stiffness matrix at the perturbed state
$[K^e]$	structural stiffness matrix at the initial state
l_p	generator length for each conical segment
L	total generator length of conical shell
$[L^j]$	matrix contributed by the integrals in equation (65) which do not contain initial displacements
$[L^j_{inc}]$	matrix contributed by the integrals in equation (65) which contain initial displacements
m	$\cos \Phi$
$[m]$	elemental mass matrix at the perturbed state
$[m^e]$	elemental mass matrix at the initial state
$[M]$	structural mass matrix at the perturbed state
$[M_e]$	transformation matrix at the initial state; also structural mass matrix at the initial state
$[M_p]$	transformation matrix at the perturbed state
n	$\sin \Phi$
$\bar{n}$	unit vector normal to the middle surface of the shell
N	total number of finite elements
p	perturbed state; also hydrostatic pressure loading
P	time dependent external applied loads
P_o	statical component of applied loads

P_t	pulsating component of applied loads
P^*	fundamental static buckling loads
$\Delta\bar{P}$	the increment in force vector
$[P]$	matrix used in formulating the elemental mass matrix
$\{q\},\{\dot{q}\},\{\ddot{q}\}$	generalized displacements, velocities, and accelerations at the perturbed state
$\{q^e\},\{\dot{q}^e\},\{\ddot{q}^e\}$	generalized displacements, velocities, and accelerations at the initial state
$\{Q\}$	generalized forces at the perturbed state
$\{Q^e\}$	generalized forces at the initial state
r	radius at any meridional distance s
r_p	radius at the nodal station p
r_{p+1}	radius at the nodal station p+1
R_1,R_2	smaller and larger radius of the truncated conical shell
s	meridional coordinates
$[s]$	stability coefficient matrix of the p^{th} element in the j^{th} harmonic
$[S]$	total structural stability coefficient matrix at the perturbed state
t	time
t_o	initial instant of time
t_1	final instant of time
$\bar{t}_s,\bar{t}_\theta$	unit vectors along the meridional direction s, and circumferential direction θ
T	kinetic energy; also period of pulsating load

$T^e, \delta T, \delta^2 T$	the initial state, first, and second variation of kinetic energy of the shell
T^p	total kinetic energy for an entire shell at the perturbed state
u, $\dot{u}$	displacement and velocity at the perturbed state along the meridional direction
u^e, $\dot{u}^e$	displacement and velocity at the initial state along the meridional direction
U^p	strain energy of the shell at the perturbed state
$U^e, \delta U, \delta^2 U$	the initial state, first, and second variation of the strain energy of the shell
v, $\dot{v}$	displacement and velocity at the perturbed state along the circumferential direction
$v^e, \dot{v}^e$	displacement and velocity at the initial state along the circumferential direction
$\bar{V}$	displacement field
$[V]$	matrix used in formulating the $[P]$ matrix
w, $\dot{w}$	displacement and velocity at the perturbed state along the direction normal to the middle surface of the shell
$w^e, \dot{w}^e$	displacement and velocity at the initial state along the direction normal to the middle surface of the shell
W^e, W^p	total potential energy of the noninertial forces at the initial and perturbed states
z	axial coordinates

α	percentage of the static buckling load which is applied statically
β	percentage of the static buckling load which is applied as the magnitude of the pulsating component of the applied loads
$\{\beta\}$	undetermined constant matrix at the perturbed state
$\{\beta^e\}$	undetermined constant matrix at the initial state
γ	integer
δ	integer; also variational notation
$\Delta( )$	incremental change in ( )
$(\epsilon_s)_L, (\epsilon_\theta)_L$	strain components which are linear in u, v, w, and their derivatives
$\epsilon_s, \epsilon_\theta, \epsilon_{s\theta}$	strain components at the initial state
$\delta\epsilon_s, \delta\epsilon_\theta, \delta\epsilon_{s\theta}$	strain components involving terms that are linear in u, v, w, and their derivatives
$\delta^2\epsilon_s, \delta^2\epsilon_\theta, \delta^2\epsilon_{s\theta}$	strain components involving terms that are quadratic in u, v, w, and their derivatives
θ	frequency of applied loads; also circumferential coordinates
$\varkappa_s, \varkappa_\theta, \varkappa_{s\theta}$	curvature changes at the initial state
$\delta\varkappa_s, \delta\varkappa_\theta, \delta\varkappa_{s\theta}$	curvature changes expressions involving terms that are linear in u, v, w, and their derivatives
$\delta^2\varkappa_s, \delta^2\varkappa_\theta, \delta^2\varkappa_{s\theta}$	curvature changes expressions involving terms that are quadratic in u, v, w, and their derivatives
μ	parameter varying from 0 to 1; also excitation parameter
ν	Poisson's ratio
ρ	mass density of the shell material

$\sum$	summation sign
$\Delta\bar{\tau}$	rotation vector
Φ	semi-vertex angle of the cone
$\Psi_s, \Psi_\theta, \Psi$	rotations along the meridional direction s, circumferential direction θ, and the normal $\bar{n}$ to the middle surface of the shell
ω	natural frequency of transverse free vibration
Ω^p	potential energy of the applied loads at the perturbed state
$\bar{\Omega}$	frequency of free vibrations of the structure loaded by the constant component of the time-dependent applied loads
$\Delta\Omega$	the increment in potential energy of the applied loads
$\Omega^e, \delta\Omega, \delta^2\Omega$	the initial state, first, and second variation of potential energy of the applied loads
$\{\ \}$	column matrix
$\{\ \}^T$	transpose of column matrix
$[\ ]$	square matrix
$[\ ]^T$	transpose of square matrix
	subscript following a comma denotes partial differentiation of the primary quantity with respect to the subscript quantity

CHAPTER I

INTRODUCTION

1.1 Statement of the Problem

During the last few decades, problems of dynamic stability of shell structures have increasingly attracted the attention of both scientists and engineers. The reason for intensifying the studies in this area is probably due to the development of missiles and rockets. These vehicles are forced to move at high speeds by rocket engines, and encounter pressure fluctuations on the vehicle structure during transition and supersonic flight (1). Pressure fluctuations in turn may cause the vehicle structure to be dynamically unstable. Thus, these problems, which have long been of theoretical interest, have recently turned out to be very important from a practical point of view.

The structural design of a typical aerospace vehicle requires that the response of the vehicle to various excitations (e.g., longitudinally excited pulsating pressures) be accurately predicted in order that the soundness and reliability of the vehicle can be assessed. Since the conical shell is extensively used as a structural component in many existing and proposed flight vehicles, the stability of the shell under the action of an external

uniform pulsating hydrostatic pressure is of great importance and will therefore be investigated in this thesis.

The results of this analysis will be depicted in the form of principal regions of dynamic instability for different shell theories, various geometrical parameters and support conditions. (An instability region can be visualized as a domain in the load-frequency space which will indicate whether or not a certain load applied at a given frequency will cause the structure to become dynamically unstable.)

1.2 Historical Sketch

The phenomenon of parametric resonance in a stretched string has long been observed. However, Rayleigh (2) was the first to give a theoretical explanation of this phenomenon. A detailed review of the literature on the theory of dynamic stability, complete through 1951, can be found in an article by E. A. Beilin and G. U. Dzhanelidze (3). One of the most comprehensive treatises in this field was presented by Bolotin (4) in his book Dynamic Stability of Elastic Systems.

In 1949 Markov (5) investigated the dynamic stability of anisotropic cylindrical shells and Oniashvilli (6) studied the dynamic stability of shallow shells in 1950. Federhofer (7), in 1954, published a paper on the dynamic stability of cylindrical shells under axial pressures.

In 1958 Bolotin (8) published several papers on the

dynamic stability of spherical shells and Bublik and Merkulov (9) studied the dynamic stability of shells filled with liquid. The question of the influence of damping on the boundaries of the regions of instability was discussed by Mettler (10) and Naumov (11).

The first paper known to the author dealing with the dynamic stability of cones appeared in 1955. In their study Alfutov and Razumeev (12) restricted the analysis to shells with small cone angles and it was assumed that the shells perform inextensional vibrations. Black (13) in 1968, employed the finite element method to study the dynamic instability of cylindrical shells. Although he used the same approach as that of the present study, his means of obtaining the structural property matrices cannot be used for the more complex geometry of a conical shell. The dynamic stability of truncated conical shells has been studied by Kornecki (14) in 1966. Kornecki assumed in his paper that the mode shapes corresponding to the practically most important parametric vibrations contain a large number of circumferential waves. No such limitation is imposed in the present study.

Most of works on dynamic stability mentioned earlier had a common characteristic in that the governing differential equations could, either exactly or approximately, be reduced to a second-order differential equation with periodic coefficients known as the Mathieu-Hill equation. For example, Brachkovskii (15) established a class of problems

that can be reduced exactly to one second-order equation by using the Galerkin method.

The idea of replacing any structure by a series of finite structural elements can be traced back several decades. The development of this concept of structural analysis began to show its versatility and ease in the application for solving the problems of plates and shells only about ten years ago.

The first application of this technique to shells which involved replacing the curved surface by flat triangular or rectangular elements had been done by Adini (16), Clough and Tocher (17), and Zienkiewicz and Cheung (18). An alternative approach for a shell of revolution which consists in replacing the shell by a set of conical segments was treated by Grafton and Strome (19). Percy et al. (20), and Dong (21) extended the method to handle laminated shells and orthotropic materials. Dong (21), Clough (17), and Navaratna (22) studied the effect of the element size on solution accuracy.

Recently, Jones and Strome (23), and Stricklin et al. (24) modified the method for a shell of revolution by using curved meridional elements rather than conical segments. To analyze a shell of arbitrary shape, Utku (25) has proposed an element stiffness matrix for a shallow triangular curved element. Webster (26) made improvements in the ring finite element analysis by extending the polynomials representing the displacements. Connor and Brebbia

(27) developed the element stiffness and nodal force matrices for a shallow shell element taking into account the effects of curvature.

The application of the finite element method to study the dynamic stability of beams, plates, and shells had been done for the first time by Brown (28), Hutt (29), and Black (13). The finite element approach using the direct stiffness method has also been employed to solve classical elastic stability problems of simple structures. Geometric stiffness matrices for simple bar elements, beam columns, and plates have been obtained by Turner et al. (30), Archer (31), Gallagher et al. (32), Argyris (33), Martin (34), Kapur and Hartz (35) and Oden (36) from purely geometric considerations. A systematic procedure to obtain the so-called geometric stiffness, or stability coefficient, and stiffness matrices for more complicated structures had been developed by Navaratna (37) through the variational approach.

1.3 Approach of This Study

In this thesis the finite element method is used to study the dynamic stability of a truncated conical shell. The original structure is replaced by a series of conical frusta as shown in Figure 1. Each conical frustum is bounded by two nodes. The displacements of the shell are described by the displacements of these nodes. Each node is assumed to have four degrees of freedom for asymmetric

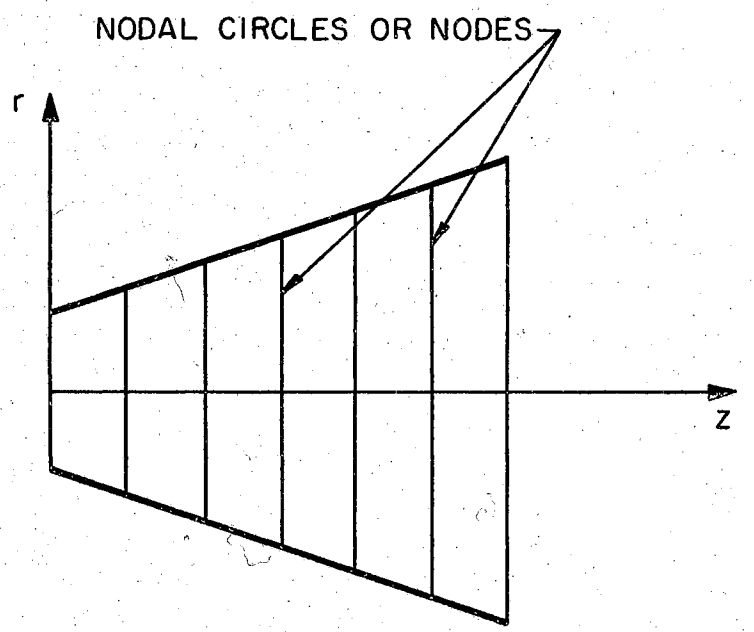

Figure 1. Discretized Shell of Revolution

deformation during buckling and three degrees of freedom for axisymmetric, torsionless, prebuckling deformation. The formulation of both stiffness and stability coefficient matrices for any discrete element is carried out using the variational principles. This yields matrices that are positive definite for prebuckling equilibrium and symmetric for the perturbation problem. Both Donnell's and Sanders' non-linear theories for thin shells are used. The mass matrix for each finite element is derived from the definition of kinetic energy. The displacement and velocity fields are assumed throughout the element for the formulation of various matrices. Finally the behavior of the entire structure is determined by introducing the compatibility condition at the node of each element.

In this study the shell is assumed to be made up of homogeneous and isotropic material that obeys Hooke's law. Further, the thickness of the shell is small in comparison with the radii of curvature, while the shell is initially perfect and all of the perturbation quantities are small.

1.4 Solution Procedure

The boundaries of the regions of dynamic instability of shells can be obtained in the following manner:

(a) Determine the equations of motion of a typical shell element;

(b) Discretize the original structure into a series of conical frusta;

(c) Assume a suitable displacement and velocity function for the above element;

(d) Derive the elemental stiffness, stability coefficient and mass matrices;

(e) Assemble the elemental matrices to obtain the equation of motion for the entire structure;

(f) Apply the boundary conditions;

(g) Calculate the natural frequency of transverse free vibration;

(h) Calculate the static buckling load;

(i) Solve for the regions of dynamic instability from the equation of motion of the entire shell.

CHAPTER II

FORMULATION OF THE CONDITIONS OF DYNAMIC INSTABILITY

2.1 Equations of the Shell Dynamics

If the shell is subjected to dynamic edge and surface loads it will, in general, experience a state of forced vibration in a configuration compatible with the nature of the driving forces and the boundary conditions. In more precise terms, except for the time dependence of this configuration, its form will be the same as that of the same shell under static loading. This state or configuration will be referred to as the initial state and is assumed to be nowhere near resonance. According to Hamilton's principle (38), the following relationship holds between two instants of time t_o and t_1:

$$\int_{t_o}^{t_1} \delta(T^e + W^e)dt = 0 \qquad (1)$$

in which

T^e = kinetic energy of the shell at the initial state, and

W^e = total potential and strain energy at the initial state.

As is well known, equation (1) is a generalization of the principle of virtual work, in which case, δT^e is interpreted as the virtual work of the inertial forces, while δW^e is the virtual work of the noninertial driving forces. It is noted here that T^e and W^e are functions of the displacements u^e, v^e, w^e and their time rate at the initial state. More specifically, T^e and W^e are functions of a set of generalized displacements $\{q^e\}$ and velocities $\{\dot{q}^e\}$.

Performing the integration in equation (1) and expressing the total potential energy W^e as the sum of the strain energy U^e and the work Ω^e done by the generalized forces $\{Q\}$ leads to the well-known Lagrange's equation for the dynamic equilibrium of the initial state:

$$\frac{d}{dt}\left(\frac{\partial T^e}{\partial \{\dot{q}^e\}}\right) - \frac{\partial}{\partial \{q^e\}} (T^e - U^e - \Omega^e) = 0 \ . \tag{2}$$

By introducing the following expressions for T^e, U^e, and Ω^e for a typical element of the shell:

$$\left.\begin{aligned} T^e &= \tfrac{1}{2}\{\dot{q}^e\}^T [m^e] \{\dot{q}^e\} \\ U^e &= \tfrac{1}{2}\{q^e\}^T [k^e] \{q^e\} \\ \Omega^e &= -\{q^e\}^T \{Q\} \end{aligned}\right\} \tag{3}$$

equation (2) is transformed to:

$$[m^e]\{\ddot{q}^e\} + [k^e]\{q^e\} = \{Q\} \tag{4}$$

in which

$[m^e]$ = elemental mass matrix of the initial state,

$[k^e]$ = elemental stiffness matrix of the initial state,

$\{q^e\}$, $\{\dot{q}^e\}$, $\{\ddot{q}^e\}$ = generalized displacements, velocities, and accelerations at the initial state respectively.

The equation of motion for the entire shell is obtained by requiring compatibility of the generalized coordinates, a process which leads to a straight-forward assemblage of total mass and stiffness matrices $[M^e]$ and $[K^e]$ from the elemental mass and stiffness matrices $[m^e]$ and $[k^e]$. These matrices describe structural properties and are time independent. Thus, the initial state of the entire shell is governed by the equation

$$[M^e]\{\ddot{q}^e\} + [K^e]\{q^e\} = \{Q\} . \qquad (5)$$

In order to investigate the dynamic stability of the initial state governed by equation (5) it is necessary to consider the stability of all neighboring configurations that satisfy the geometric edge conditions of the shell. This is done by perturbing the initial state infinitesimally from u^e, v^e, w^e to (u^e+u), (v^e+v), (w^e+w). These new deformation states will be referred to as the perturbed states (p).

The equation of perturbed motion is derived from Hamilton's principle expressed as

$$\int_{t_o}^{t_1} \delta(T^p + W^p)dt = 0 \qquad (6)$$

in which

T^p = kinetic energy of the shell at the perturbed state

$= T^r + \delta T + \frac{1}{2}\delta^2 T + \ldots$, and

W^p = potential energy of the noninertial forces at the perturbed state

$= -(U^p + \Omega^p)$.

In the above:

U^p = strain energy of the shell at the perturbed state

$= U^e + \delta U + \frac{1}{2}\delta^2 U + \ldots$, and

Ω^p = potential energy of the applied loads at the perturbed state

$= \Omega^e + \delta\Omega + \frac{1}{2}\delta^2\Omega + \ldots$

where

T^e, U^e, Ω^e = kinetic, strain and potential energy, respectively, of the applied loads at the initial state, which is a state of dynamic equilibrium,

δT, δU, $\delta\Omega$ = the first variation of kinetic, strain and potential energy, respectively, and

$\frac{1}{2}\delta^2 T$, $\frac{1}{2}\delta^2 U$, $\frac{1}{2}\delta^2\Omega$ = the second variation of kinetic, strain and potential energy, respectively.

Equation (6) then becomes:

$$\delta \int_{t_o}^{t_1} (T^p - U^p - \Omega^p)\,dt = 0 \,. \tag{7}$$

Substituting the variational forms of T^p, U^p and Ω^p in equation (7), and by retaining infinitesimals up to the second order, the following is obtained

$$\delta \int_{t_o}^{t_1} [(T^e - U^e - \Omega^e) + (\delta T - \delta U - \delta\Omega) + \tfrac{1}{2}(\delta^2 T - \delta^2 U - \delta^2\Omega)]\,dt = 0 \,. \tag{8}$$

During the variation of the p state the variables of the e state are held constant; therefore:

$$\delta \int_{t_o}^{t_1} (T^e - U^e - \Omega^e)dt = 0 \ . \qquad (9)$$

Since the p state is also a state of dynamic equilibrium, the first variation of the p state must satisfy Hamilton's equation:

$$\delta \int_{t_o}^{t_1} (\delta T - \delta U - \delta \Omega)dt = 0 \ . \qquad (10)$$

From equations (8), (9), and (10), it follows that

$$\delta \int_{t_o}^{t_1} \tfrac{1}{2}(\delta^2 T - \delta^2 U - \delta^2 \Omega)dt = 0 . \qquad (11)$$

This again leads to the Lagrange's equation of motion in terms of the generalized perturbed displacements and velocities $\{q\}$ and $\{\dot{q}\}$ respectively:

$$\frac{d}{dt}\left(\frac{\partial T^{(2)}}{\partial \{\dot{q}\}}\right) - \frac{\partial}{\partial \{q\}} (T^{(2)} - U^{(2)} - \Omega^{(2)}) = 0 \qquad (12)$$

where

$T^{(2)} = \tfrac{1}{2}\delta^2 T$

$U^{(2)} = \tfrac{1}{2}\delta^2 U$

$\Omega^{(2)} = \tfrac{1}{2}\delta^2 \Omega$

$\{q\}$ = perturbed generalized displacements, and

$\{\dot{q}\}$ = perturbed generalized velocities.

It should be kept in mind that $T^{(2)}$ is, in general, a function of both generalized displacements and velocities

whereas $U^{(2)}$ and $\Omega^{(2)}$ are functions of only generalized displacements. Since, in this work, $T^{(2)}$ is a function of only generalized velocities,

$$\frac{\partial T^{(2)}}{\partial \{q\}} = 0 \ . \tag{13}$$

The Lagrange's equation (12) then takes the form:

$$\frac{d}{dt}\left(\frac{\partial T^{(2)}}{\partial \{\dot{q}\}}\right) + \frac{\partial U^{(2)}}{\partial \{q\}} + \frac{\partial \Omega^{(2)}}{\partial \{q\}} = 0 \ . \tag{14}$$

The expressions for $T^{(2)}$ and $U^{(2)} + \Omega^{(2)}$ can be written in the following form:

$$T^{(2)} = \tfrac{1}{2}\{\dot{q}\}^T [m]\{\dot{q}\} \ ,$$

and

$$U^{(2)}+\Omega^{(2)} = \tfrac{1}{2}\{q\}^T [k]\{q\} - \frac{P}{2}\{q\}^T [s]\{q\} \ . \tag{15}$$

The term which has P as its coefficient in the expression for $U^{(2)}+\Omega^{(2)}$ above is referred to as the geometric stiffness or stability coefficient matrix. It accounts for the contribution to the elemental stiffness matrix resulting from the change in geometry of the shell element. Furthermore, this term depends on the nature of the externally applied forces and the manner in which these forces are affected by the change in geometry. If the forces are in the form of edge forces, $\frac{\partial \Omega^{(2)}}{\partial \{q\}} = 0$, the [s] matrix depends only on the equilibrium strains prior to instability. On the other hand if the forces are in the form of a lateral pressure, the contribution of $\frac{\partial \Omega^{(2)}}{\partial \{q\}}$ can be added to the [s] matrix. A detailed examination of the construction and make up of the different

matrices will be shown in Chapter III.

Therefore, equation (14) becomes:

$$[m]\{\ddot{q}\} + [k]\{q\} - P[s]\{q\} = 0 \qquad (16)$$

in which

[m] = elemental mass matrix of the perturbed state,

[k] = elemental stiffness matrix of the perturbed state,

[s] = elemental stability coefficient matrix of the perturbed state, and

P = time-dependent external applied loads.

Equation (16) is the equation of perturbed motion of a typical element in terms of the mass, stiffness, and stability coefficient matrices of that element. The equation of motion of the entire structure is obtained by assembling all the finite elements to form the complete structure. Denoting the assembled mass, stiffness, and stability coefficient matrices by [M], [K] and [S] and performing the mentioned operation results in:

$$[M]\{\ddot{q}\} + [K]\{q\} - P[S]\{q\} = 0 \qquad (17)$$

which is the equation of perturbed motion for the entire structure.

2.2 Regions of Dynamic Instability

The time-dependent applied loads P(t) in equation (17) will be represented in the following form:

$$P(t) = P_o + P_t \cos \theta t \qquad (18)$$

in which P_o and P_t are statical and pulsating components

of the applied loads whose frequency is θ. Substituting equation (18) into equation (17) yields:

$$[M]\{\ddot{q}\} - (P_o + P_t \cos \theta t)[S]\{q\} + [K]\{q\} = 0. \quad (19)$$

By introducing the concept of pulsating parametric loading, the theory of the dynamic stability of elastic systems can be reduced to the study of vibrations caused by parametric loading with respect to certain forms of deformations. Such a loading is characterized by the fact that it is contained as a parameter in the equation of perturbed motion.

Theoretical studies (4), (39) and experimental verification (40) have revealed that under some definite values of the ratio θ/ω of the frequency of applied loads θ and the natural frequency of transverse free vibration ω, the initial state of the structure becomes unstable. The transition from the initially stable state to the perturbed unstable one occurs when it is possible for the system of equations (19) to have periodic solutions with periods $T = \frac{2\pi}{\theta}$ or $2T = \frac{4\pi}{\theta}$. This transition then provides the boundary between stable and unstable solutions, or as commonly termed, regions of stability and instability. Two solutions with the same period confine the region of instability, and two solutions with different periods confine the regions of stability.

Since the generalized displacements and accelerations in equation (19) are functions of position and time, the solution of equation (19), for a period 2T, may be written

as a series

$$\{q(t)\} = \sum_{k=1,3,5,\ldots}^{\infty} \left\{\{a_k\} \sin\frac{k\theta t}{2} + \{b_k\}\cos\frac{k\theta t}{2}\right\} \qquad (20)$$

where $\{a_k\}$ and $\{b_k\}$ are independent of time. The series (20) is obviously equivalent to n sets of Fourier series for the components of displacements $\{q(t)\}$.

Substituting equation (20) in equation (19) and comparing coefficients of $\sin\frac{k\theta t}{2}$ and $\cos\frac{k\theta t}{2}$ gives the following system of matrix equations:

$$[[K] - P_o[S] + \tfrac{1}{2}P_t[S] - \frac{\theta^2}{4}[M]]\{a_1\} - \tfrac{1}{2}P_t[S]\{a_3\} = 0$$

$$[[K] - P_o[S] - \frac{k^2\theta^2}{4}[M]\{a_k\} - \tfrac{1}{2}P_t[S](\{a_{k-2}\} + \{a_{k+2}\}) = 0$$

$$(k = 3, 5, 7, \ldots) \qquad (21)$$

and,

$$[[K] - P_o[S] - \tfrac{1}{2}P_t[S] - \frac{\theta^2}{4}[M]]\{b_1\} - \tfrac{1}{2}P_t[S]\{b_3\} = 0$$

$$[[K] - P_o[S] - \frac{k^2\theta^2}{4}[M]]\{b_k\} - \tfrac{1}{2}P_t[S](\{b_{k-2}\} + \{b_{k+2}\}) = 0$$

$$(k = 3, 5, 7, \ldots)\ . \qquad (22)$$

The condition for the existence of solutions with a period $\frac{4\pi}{\theta}$ has, after the two conditions are combined under the $\pm$ sign, the form:

$$\begin{vmatrix} [K]-(P_o\pm\frac{1}{2}P_t)[S]-\frac{\theta^2}{4}[M] & -\frac{1}{2}P_t[S] & 0 & \cdot \\ -\frac{1}{2}P_t[S] & [K]-P_o[S]-\frac{9}{4}\theta^2[M] & -\frac{1}{2}P_t[S] & \cdot \\ 0 & -\frac{1}{2}P_t[S] & [K]-P_o[S]-\frac{25}{4}\theta^2[M] & \cdot \\ \cdot & \cdot & \cdot & \cdot \end{vmatrix} = 0 \qquad (23)$$

If the series

$$\{q(t)\} = \tfrac{1}{2}\{b_o\} + \sum_{k=2,4,6,\ldots}^{\infty} \left\{\{a_k\} \sin \frac{k\theta t}{2} + \{b_k\} \cos \frac{k\theta t}{2}\right\} \qquad (24)$$

is substituted into equation (19), the following conditions for the existence of solutions with a period $\frac{2\pi}{\theta}$ are obtained:

$$\begin{vmatrix} [K]-P_o[S]-\theta^2[M] & -\tfrac{1}{2}P_t[S] & 0 & \cdot \\ -\tfrac{1}{2}P_t[S] & [K]-P_o[S]-4\theta^2[M] & -\tfrac{1}{2}P_t[S] & \cdot \\ 0 & -\tfrac{1}{2}P_t[S] & [K]-P_o[S]-16\theta^2[M] & \cdot \\ \cdot & \cdot & \cdot & \cdot \end{vmatrix} = 0 \qquad (25)$$

and

$$\begin{vmatrix} [K]-P_o[S] & -P_t[S] & 0 & 0 & \cdot \\ -\tfrac{1}{2}P_t[S] & [K]-P_o[S]-\theta^2[M] & -\tfrac{1}{2}P_t[S] & 0 & \cdot \\ 0 & -\tfrac{1}{2}P_t[S] & [K]-P_o[S]-4\theta^2[M] & -\tfrac{1}{2}P_t[S] & \cdot \\ 0 & 0 & -\tfrac{1}{2}P_t[S] & [K]-P_o[S]-16\theta^2[M] & \cdot \\ \cdot & \cdot & \cdot & \cdot & \cdot \end{vmatrix} = 0 \qquad (26)$$

For an exact calculation of the regions of instability, the equations (23), (25) and (26) have to be solved. However, it has been observed both theoretically and experimentally (4) that it is sufficiently accurate from an engineering standpoint to calculate only the principal region of dynamic instability which corresponds to k=1. Hence a good approximate expression for the boundaries of the principal regions of instability is obtained by equating to zero the determinant of the first matrix element

in the principal diagonal of the matrix equation (23):

$$|[K] - (P_o \pm \tfrac{1}{2}P_t)[S] - \frac{\theta^2}{4}[M]| = 0 \ . \qquad (27)$$

This approximation is equivalent to the assumption that the periodic solutions on the boundaries of the principal regions of instability are the harmonic functions:

$$\{q(t)\} = \{a\} \sin \frac{\theta t}{2} + \{b\} \cos \frac{\theta t}{2} \ . \qquad (28)$$

2.3 Degenerate Cases

For the purpose of constructing the regions of dynamic stability and instabilities from equation (27), consider the following limiting cases:

(a) For free transverse vibrations P_o and P_t vanish and equation (19) becomes

$$[M] \{\ddot{q}\} + [K] \{q\} = 0 \ . \qquad (29)$$

For harmonic vibrations of the form

$$\{q\} = \{a_k\} \sin \omega t \ , \qquad (30)$$

where $\{a_k\}$ are independent of time, the frequency determinant becomes

$$|[K] - \omega^2[M]| = 0 \ . \qquad (31)$$

(b) For the case of static buckling, $\{\ddot{q}\}$ and P_t are zero and equation (19) reduces to

$$([K] - P_o[S]) \{q\} = 0 \ . \qquad (32)$$

Static instability occurs when the following determinant vanishes:

$$|[K] - P_o[S]| = 0 \ . \qquad (33)$$

Referring back to equation (19) for the dynamic stability of undamped system, let P_o and P_t be expressed by

$$\begin{aligned} P_o &= \alpha P^* \\ P_t &= \beta P^* \end{aligned} \tag{34}$$

where P^* is the fundamental static buckling load obtained from equation (33), and α and β are proportionality factors. Then the governing differential equation (19) becomes

$$[M]\{\ddot{q}\} - P^*(\alpha+\beta\cos\theta t)[S]\{q\} + [K]\{q\} = 0 \tag{35}$$

and the associated characteristic equation becomes

$$\left|[K] - (\alpha \pm \tfrac{1}{2}\beta)P^*[S] - \frac{\theta^2}{4}[M]\right| = 0 \ . \tag{36}$$

CHAPTER III

DERIVATION OF STIFFNESS, STABILITY COEFFICIENT, AND MASS MATRICES

3.1 General

The regions of dynamic instability can be constructed from equation (36) of the previous chapter for the strucural system at hand. This can be done once the [K], [S], and [M] matrices are established for the conical shell shown in Figure 2, under the action of external uniform pressure and edge forces that change harmonically in time according to equation (18) of the previous chapter.

Employing the finite element procedure, the original shell is replaced by a series of conical frusta connected at nodal circles. The stiffness properties of a typical conical frustum are developed in the following sections from energy considerations.

3.2 Basic Assumptions

In the formulation of stiffness and stability coefficient matrices for any typical element, nonlinear theory of thin shells will be consulted together with the following assumptions for linearly elastic thin shells:

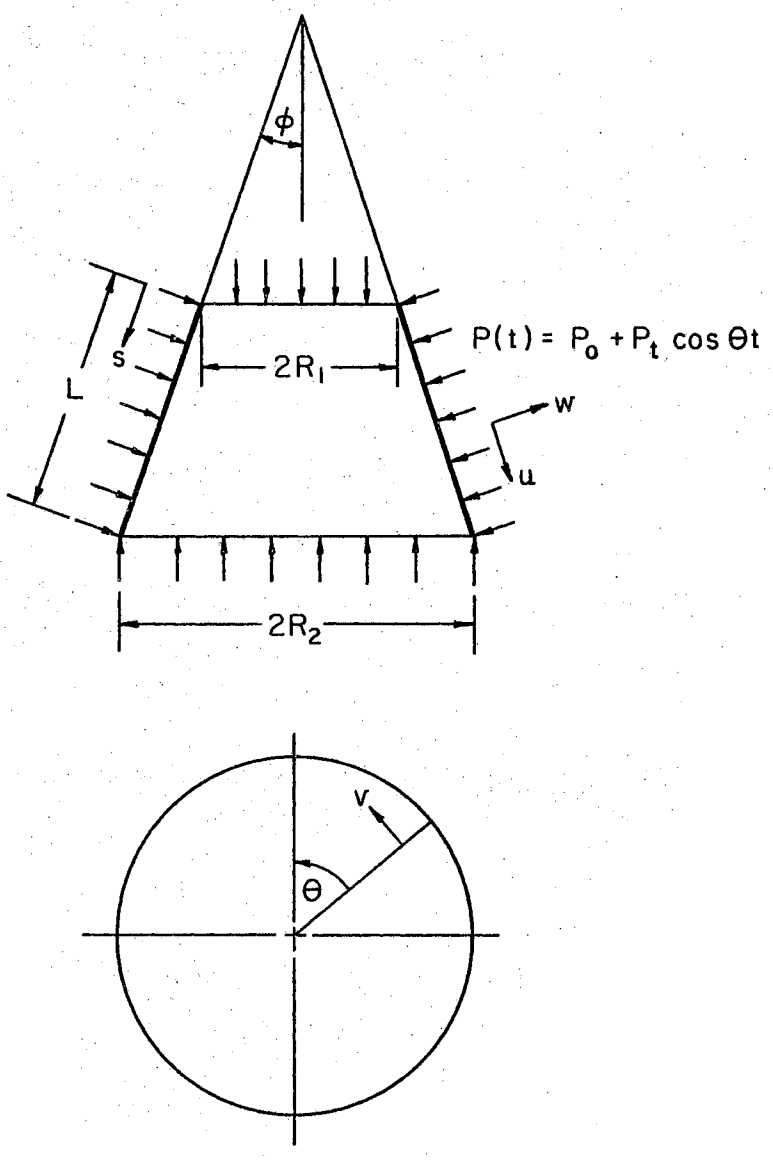

Figure 2. A Truncated Conical Shell Under the Action of an External Uniform Load That Changes Harmonically in Time

(1) the shell is made of isotropic and homogeneous material that obeys Hooke's law; (2) the shell thickness is uniform and is small in comparison with the radii of curvature; (3) the Kirchhoff-Love hypothesis for thin shells is applicable; (4) both membrane and bending stresses are present and vary throughout the shell; (5) all of the perturbation quantities are infinitesimals; and (6) the shell and the loading on it are rotationally symmetric.

3.3 Second Variation of Strain Energy

In the variational approach of the theory of buckling where the second variation is to be determined, it is necessary to retain quadratic terms in the strain-displacement relations. Donnell's non-linear theory (41) of thin shells is used for all derivations in this chapter owing to its simplicity as contrasted with the complexity of the more complete Sanders' theory (41) which is presented in Appendix A. The final form of the derivations in terms of elements of stiffness and stability coefficient matrix for both Donnell's and Sanders' theory are tabulated in various appendices. The expressions for strain-displacement following Donnell's nonlinear theory are:

$$\left.\begin{aligned}
\varepsilon_s &= u^e{}_{,s} + \tfrac{1}{2}(w^e{}_{,s})^2 \\
\varepsilon_\theta &= \frac{1}{r}(nu^e + v^e{}_{,\theta} + mw^e) + \frac{1}{2r^2}(w^e{}_{,\theta})^2 \\
\varepsilon_{s\theta} &= \frac{1}{2r}(rv^e{}_{,s} + u^e{}_{,\theta} - nv^e) + \frac{1}{2r} w^e{}_{,s}\, w^e{}_{,\theta} \\
\kappa_s &= - w^e{}_{,ss}
\end{aligned}\right\} \qquad (37)$$

$$\left.\begin{aligned} \varkappa_\theta &= -\frac{1}{r}\left(\frac{1}{r}\, w^e{}_{,\theta\theta} + n w^e{}_{,s}\right) \\ \varkappa_{s\theta} &= -\frac{1}{r}\left(w^e{}_{,s\theta} - \frac{1}{r}\, n w^e{}_{,\theta}\right) \end{aligned}\right\} \quad (37)(\text{Cont'd})$$

In the foregoing expressions (37), the various terms represent:

u^e, v^e, w^e = initial displacements in the meridional, circumferential, and normal direction to the middle surface of the shell, respectively,

m = $\cos \Phi$,

n = $\sin \Phi$,

Φ = semi-vertex angle of the cone,

r = radius at any distance s,

s, θ = meridional and circumferential coordinates,

and the s, θ subscripts following the commas on u^e, v^e, and w^e denote partial derivatives.

Let (u^e, v^e, w^e) be the displacement vector that defines the given initial configuration before instability occurs. Let (u, v, w) be an incremental virtual displacement vector. Then the total displacement vector is (u^e+u, v^e+v, w^e+w). Substituting the total displacement vector into equations (37) and, with the application of assumption (6), p. 23, $v^e = w^e{}_{,\theta} = 0$, the following is obtained:

$$\left.\begin{aligned} \varepsilon_s + \Delta\varepsilon_s &= u^e{}_{,s} + u_{,s} + \tfrac{1}{2}(w^2{}_{,s} + 2w^e{}_{,s}\, w_{,s}) \\ \varepsilon_\theta + \Delta\varepsilon_\theta &= \frac{1}{r}(nu^e + mw^e) + \frac{1}{r}(nu + v_{,\theta} + mw) + \frac{1}{r^2}\, w^2{}_{,\theta} \\ \varepsilon_{s\theta} + \Delta\varepsilon_{s\theta} &= \frac{1}{2r}(rv_{,s} + u_{,\theta} - nv) + \frac{1}{2r}\, w^e{}_{,s}\, w_{,\theta} + \frac{1}{r}\, w_{,s}\, w_{,\theta} \\ \varkappa_s + \Delta\varkappa_s &= -(w^e{}_{,ss} + w_{,ss}) \\ \varkappa_\theta + \Delta\varkappa_\theta &= -\frac{1}{r^2}(w^e{}_{,\theta\theta} + w_{,\theta\theta}) - \frac{n}{r}(w^e{}_{,s} + w_{,s}) \end{aligned}\right\} \quad (38)$$

and

$$\kappa_{s\theta} + \Delta\kappa_{s\theta} = -\frac{1}{r}\left(w^{e}{}_{,s\theta} + w_{,s\theta}\right) + \frac{n}{r^2}\left(w^{e}{}_{,\theta} + w_{,\theta}\right) \quad (38)$$

(Cont'd)

where $\Delta\varepsilon_s$, $\Delta\varepsilon_\theta$, $\Delta\varepsilon_{s\theta}$, $\Delta\kappa_s$, $\Delta\kappa_\theta$ and $\Delta\kappa_{s\theta}$ are the incremental strains and curvature changes due to the virtual, or perturbation, displacement vector (u, v, w).

Expanding $\Delta\varepsilon_s$, $\Delta\varepsilon_\theta$, $\Delta\varepsilon_{s\theta}$, $\Delta\kappa_s$, $\Delta\kappa_\theta$ and $\Delta\kappa_{s\theta}$ gives:

$$\left.\begin{aligned}
\Delta\varepsilon_s &= \delta\varepsilon_s + \tfrac{1}{2}\delta^2\varepsilon_s + \cdots \\
\Delta\varepsilon_\theta &= \delta\varepsilon_\theta + \tfrac{1}{2}\delta^2\varepsilon_\theta + \cdots \\
\Delta\varepsilon_{s\theta} &= \delta\varepsilon_{s\theta} + \tfrac{1}{2}\delta^2\varepsilon_{s\theta} + \cdots \\
\Delta\kappa_s &= \delta\kappa_s + \tfrac{1}{2}\delta^2\kappa_s + \cdots \\
\Delta\kappa_\theta &= \delta\kappa_\theta + \tfrac{1}{2}\delta^2\kappa_\theta + \cdots \\
\Delta\kappa_{s\theta} &= \delta\kappa_{s\theta} + \tfrac{1}{2}\delta^2\kappa_{s\theta} + \cdots
\end{aligned}\right\} \quad (39)$$

where $\delta\varepsilon_s$, $\delta\varepsilon_\theta$, $\delta\varepsilon_{s\theta}$, $\delta\kappa_s$, $\delta\kappa_\theta$ and $\delta\kappa_{s\theta}$ are linear forms in u, v and w and their derivatives, and $\delta^2\varepsilon_s$, $\delta^2\varepsilon_\theta$, $\delta^2\varepsilon_{s\theta}$, $\delta^2\kappa_s$, $\delta^2\kappa_\theta$ and $\delta^2\kappa_{s\theta}$ are quadratic terms in the same variables. Hence, by equations (38) and (39) we get:

$$\left.\begin{aligned}
\varepsilon_s &= u^{e}{}_{,s} \\
\delta\varepsilon_s &= u_{,s} + w^{e}{}_{,s}\, w_{,s} \\
\delta^2\varepsilon_s &= w^{2}{}_{,s} \\
\varepsilon_\theta &= \frac{1}{r}(nu^{e} + mw^{e}) \\
\delta\varepsilon_\theta &= \frac{1}{r}(nu + v_{,\theta} + mw) \\
\delta^2\varepsilon_\theta &= \frac{1}{r^2}\, w^{2}{}_{,\theta} \\
\varepsilon_{s\theta} &= 0 \\
\delta\varepsilon_{s\theta} &= \frac{1}{2r}(rv_{,s} + u_{,\theta} - nv) + \frac{1}{2r}\, w^{e}{}_{,s}\, w_{,\theta} \\
\delta^2\varepsilon_{s\theta} &= \frac{1}{r}\, w_{,s}\, w_{,\theta} \\
\kappa_s &= -\, w^{e}{}_{,ss} \\
\delta\kappa_s &= -\, w_{,ss}
\end{aligned}\right\} \quad (40)$$

$$
\left.
\begin{aligned}
\delta^2\kappa_s &= 0 \\
\kappa_\theta &= -\frac{1}{r}\left(\frac{1}{r}w^e{}_{,\theta\theta} + nw^e{}_{,s}\right) \\
\delta\kappa_\theta &= -\frac{1}{r}\left(\frac{1}{r}w_{,\theta\theta} + nw_{,s}\right) \\
\delta^2\kappa_\theta &= 0 \\
\kappa_{s\theta} &= -\frac{1}{r}\left(w^e{}_{,s\theta} - \frac{n}{r}w^e{}_{,\theta}\right) \\
\delta\kappa_{s\theta} &= -\frac{1}{r}\left(w_{,s\theta} - \frac{n}{r}w_{,\theta}\right) \\
\text{and} \quad \delta^2\kappa_{s\theta} &= 0
\end{aligned}
\right\} \qquad (40)\text{(Cont'd)}
$$

At any instant of time, the total strain energy of the shell is given by

$$U = \frac{C}{2}\iint (\epsilon^2{}_s + \epsilon^2{}_\theta + 2\nu\epsilon_s\epsilon_\theta + 2(1-\nu)\epsilon^2{}_{s\theta})rd\theta ds$$

$$+ \frac{D}{2}\iint (\kappa^2{}_s + \kappa^2{}_\theta + 2\nu\kappa_s\kappa_\theta + 2(1-\nu)\kappa^2{}_{s\theta})rd\theta ds\,, \qquad (41)$$

where

$$C = \frac{Eh}{1-\nu^2}\,,$$

$$D = \frac{Eh}{12(1-\nu^2)}\,,$$

E = Young's modulus of elasticity,

h = thickness of the shell, and

ν = Poisson's ratio.

Substitution of $\epsilon_s + \Delta\epsilon_s$, $\epsilon_\theta + \Delta\epsilon_\theta$, $\epsilon_{s\theta} + \Delta\epsilon_{s\theta}$, $\kappa_s + \Delta\kappa_s$, $\kappa_\theta + \Delta\kappa_\theta$ and $\kappa_{s\theta} + \Delta\kappa_{s\theta}$ for ϵ_s, ϵ_θ, $\epsilon_{s\theta}$, κ_s, κ_θ and $\kappa_{s\theta}$ in equation (41) yields

$$\begin{aligned}
U + \Delta U = \frac{C}{2}\iint [&(\epsilon_s + \delta\epsilon_s + \tfrac{1}{2}\delta^2\epsilon_s)^2 + (\epsilon_\theta + \delta\epsilon_\theta + \tfrac{1}{2}\delta^2\epsilon_\theta)^2 \\
&+ 2\nu(\epsilon_s + \delta\epsilon_s + \tfrac{1}{2}\delta^2\epsilon_s)(\epsilon_\theta + \delta\epsilon_\theta + \tfrac{1}{2}\delta^2\epsilon_\theta) \\
&+ 2(1-\nu)(\epsilon_{s\theta} + \delta\epsilon_{s\theta} + \tfrac{1}{2}\delta^2\epsilon_{s\theta})^2]\, rd\theta ds +
\end{aligned}$$

$$+ \frac{D}{2}\iint [(\varkappa_s+\delta\varkappa_s)^2+(\varkappa_\theta+\delta\varkappa_\theta)^2+2(1-\nu)(\varkappa_s+\delta\varkappa_s)(\varkappa_\theta+\delta\varkappa_\theta)$$

$$+ 2(1-\nu)(\varkappa_{s\theta}+\delta\varkappa_{s\theta})^2]\, r\,d\theta ds \,. \qquad (42)$$

Now $\Delta U = \delta U + \frac{1}{2}\delta^2 U + \ldots$, where δU is the integral of a linear form in u, v, w and their derivatives, $\delta^2 U$ is the integral of a quadratic form in u, v, w and their derivatives, and so on. Consequently:

$$\tfrac{1}{2}\delta^2 U = \iint [(\delta\epsilon_s)^2+\epsilon_s\delta^2\epsilon_s+(\delta\epsilon_\theta)^2+\epsilon_\theta\delta^2\epsilon_\theta+\nu(\epsilon_s\delta^2\epsilon_\theta+2\delta\epsilon_s\delta\epsilon_\theta$$

$$+ \epsilon_\theta\delta^2\epsilon_s)+2(1-\nu)(\delta\epsilon_{s\theta})^2]\, r\,d\theta ds$$

$$+ \frac{D}{2}\iint [(\delta\varkappa_s)^2+(\delta\varkappa_\theta)^2+2\nu\delta\varkappa_s\delta\varkappa_\theta+2(1-\nu)(\delta\varkappa_{s\theta})^2]\, r\,d\theta ds \qquad (43)$$

where

$\delta^2 U$ = second variation of strain energy for an entire shell.

Substituting equations (40) into equation (43) and neglecting quadratic terms in u^e, v^e and w^e as compared to unity, we get:

$$\tfrac{1}{2}\delta^2 U = \frac{C}{2}\iint[\{u^2{}_{,s}+\frac{1}{r^2}(nu+v_{,\theta}+mw)^2+\frac{2\nu}{r}(nuu_{,s}+u_{,s}v_{,\theta}+mu_{,s}w)$$

$$+ \frac{(1-\nu)}{2r^2}(rv_{,s}+u_{,\theta}-nv)^2\}+\{2w^e{}_{,s}u_{,s}w_{,s}+u^e{}_{,s}w^2{}_{,s}$$

$$+ \frac{1}{r^3}(nu^e+mw^e)w^2{}_{,\theta}+\frac{\nu}{r^2}u^e{}_{,s}w^2{}_{,\theta}+\frac{\nu}{r}(nu^e+mw^e)w^2{}_{,s}$$

$$+ \frac{2\nu w^e{}_{,s}}{r}(nuw_{,s}+v_{,\theta}w_{,s}+mww_{,s})+\frac{(1-\nu)}{r^2}w^e{}_{,s}(rv_{,s}w_{,\theta}$$

$$+ u_{,\theta}w_{,\theta}-nvw_{,\theta})\}]\, r\,d\theta ds +$$

$$+ \frac{D}{2} \iint [w^2_{,ss} + \left(\frac{1}{r^2} w_{,\theta\theta} + \frac{n}{r} w_{,s}\right)^2 + 2\nu \left(\frac{1}{r^2} w_{,ss} w_{,\theta\theta} + \frac{n}{r} w_{,s} w_{,ss}\right)$$

$$+ 2(1-\nu) \left(\frac{1}{r} w_{,s\theta} - \frac{n}{r^2} w_{,\theta}\right)^2] \, r d\theta ds \, . \qquad (44)$$

The initial displacements u^e, v^e and w^e in equation (44) are obtained through the solving of the equations of static equilibrium which in turn can be formulated by the principle of stationary total potential energy, i.e., $\delta(U^e + \Omega^e) = 0$. Thus u^e, v^e, w^e may in fact be taken as the static equilibrium displacements. That this is so should be clear when one considers that expression (44) is intended to yield the stiffness matrix which is a property of the structure, i.e., it is time independent.

The details of solving for the equilibrium displacements for the finite element representation of the shell is discussed in Sections 3.6.1 and 3.6.2.

3.4 Second Variation of Potential Energy of External Loads

For a shell loaded axially or torsionally at its ends, the change in potential energy is a linear function of the end displacements and therefore the second variation of potential energy of external loads $\delta^2\Omega$ is equal to zero. But when the same shell is subjected to loads which are distributed, the change in potential energy is a function of both linear and second degree displacements. In such a case the total potential energy of the entire shell will be $\delta^2 U + \delta^2\Omega$, owing to a significant contribution of $\delta^2\Omega$. In

this study the distributed loadings are restricted to hydrostatic pressure loadings which vary with the deformation in such a manner that the load always remains perpendicular to the surface with constant magnitude per unit of undeformed area. The work done by hydrostatic pressure depends only on the change of volume of the shell material under investigation. An expression for $\delta^2\Omega$ due to a hydrostatic pressure is derived. This is done without regard for the time dependence of the applied pressure.

Let $\mu\bar{V}$ be the perturbation displacement vector at any time between equilibrium state e and perturbed state p. The condition $\mu = 0$ corresponds to state e and $\mu = 1$ to state p. A small rotation vector, $\Delta\bar{\tau}$, from the initial to intermediate state defined by $\mu\bar{V}$ is given by:

$$\Delta\bar{\tau} = \mu(\psi_s \bar{t}_s + \psi_\theta \bar{t}_\theta + \psi\bar{n}) \tag{45}$$

where ψ_s, ψ_θ and ψ are rotations along the meridional direction s, circumferential direction θ, and the normal n to the middle surface and where $\bar{t}_s$, $\bar{t}_\theta$, $\bar{n}$ are unit vectors along the s, θ and n directions, respectively.

The force increment $\Delta\bar{P}$, due to this rotation, on a deformed elemental area $[1+\mu\{(\epsilon_s)_L+(\epsilon_\theta)_L\}]dA$ is

$$\Delta\bar{P} = P\Delta\bar{\tau}[1+\mu\{(\epsilon_s)_L+(\epsilon_\theta)_L\}]dA$$

or
$$\Delta\bar{P} = P\mu(\psi_s \bar{t}_s+\psi_\theta \bar{t}_\theta+\psi\bar{n})[1+\mu\{(\epsilon_s)_L+(\epsilon_\theta)_L\}]\, r\,d\theta\,ds \tag{46}$$

where

P = hydrostatic pressure loading,

μ = parameter varying from 0 to 1,

$\mu\{(\varepsilon_s)_L+(\varepsilon_\theta)_L\}dA$ = increment of elemental area dA after deformation has occurred,

$(\varepsilon_s)_L, (\varepsilon_\theta)_L$ = strain components which are linear in u, v, w and their derivatives, and

dA = elemental area prior to deformation.

Two kinds of approximations can be introduced:

(1) Following Donnell's theory, which is a special case of Sanders' theory (41), the rotation around the normal ψ to the middle surface of the shell can reasonably be approximated as zero, i.e., $\psi = 0$.

(2) Using Sanders' nonlinear theories for thin shells (41), a more realistic and practical assumption of small strains and moderately small rotations is made in order to simplify the very complicated exact theory. The equivalent mathematical representation for this assumption is $\mu\psi \approx 1$.

Equation (46) is therefore reduced to

$$\Delta\bar{P} = P\mu(\psi_s\bar{t}_s+\psi_\theta\bar{t}_\theta)[1+\mu\{(\varepsilon_s)_L+(\varepsilon_\theta)_L\}]\, rd\theta ds \qquad (47)$$

for $\psi = 0$, and

$$\Delta\bar{P} = P\mu(\psi_s\bar{t}_s+\psi_\theta\bar{t}_\theta+\frac{1}{\mu}\bar{n})[1+\mu\{(\varepsilon_s)_L+(\varepsilon_\theta)_L\}]\, rd\theta ds \qquad (48)$$

for $\mu\psi \approx 1$ where, for Sanders' theory,

$$\psi_s = -w_{,s}$$

$$\psi_\theta = -\frac{1}{r}(w_{,\theta} - v\cos\Phi^*)$$

$$(\varepsilon_s)_L = u_{,s}$$

$$(\varepsilon_\theta)_L = \frac{1}{r}(nu + v_{,\theta} + w\cos\Phi)$$

The strain-displacement relations for Donnell's theory are obtained from the expressions for Sanders' theory by eliminating the terms marked with an asterisk (*).

The increment in potential energy $\Delta\Omega$, is given by

$$\Delta\Omega = -\int_0^1 d\mu \iint (\Delta\bar{P} \cdot \bar{V})\, r\,d\theta ds \tag{49}$$

where

$$\bar{V} = u\bar{t}_s + v\bar{t}_\theta + w\bar{n} .$$

Substituting γ_s, γ_θ, $(\epsilon_s)_L$ and $(\epsilon_\theta)_L$ into equations (47) and (48) and also retaining only the linear terms in u, v, w and their derivatives, we get from equation (49):

$$\Delta\Omega = -\frac{P}{2} \iint \left\{ - uw_{,s} - \frac{1}{r} vw_{,\theta} \right\} r\,d\theta ds \tag{50}$$

for Donnell's theory, and

$$\Delta\Omega = -\frac{P}{2} \iint \left[-uw_{,s} - \frac{v}{r}(w_{,\theta} - mv) + \left\{ 2 + u_{,s} + \frac{1}{r}(nu + v_{,\theta} + mw) \right\} w \right] r\,d\theta ds \tag{51}$$

for Sanders' theory.

As before

$$\Delta\Omega = \delta\Omega + \tfrac{1}{2}\delta^2\Omega + \cdots \tag{52}$$

where

$\delta\Omega$ = integral containing linear terms in u, v, w and their derivatives, and

$\delta^2\Omega$ = integral containing quadratic terms for the same variables.

Consequently,

$$\tfrac{1}{2}\delta^2\Omega = -\frac{P}{2} \iint \left\{ -uw_{,s} - \frac{1}{r} vw_{,\theta} \right\} r\,d\theta ds \tag{53}$$

for Donnell's theory, and

$$\tfrac{1}{2}\delta^2\Omega = -\frac{P}{2}\iint[-uw_{,s} - \frac{v}{r}(w_{,\theta}-mv)+wu_{,s}+\frac{w}{r}(nu+v_{,\theta}+mw)]rd\theta ds \tag{54}$$

for Sanders' theory, where

$\delta^2\Omega$ = second variation of the potential energy of external load which in this case is the hydrostatic pressure loading.

3.5 Second Variation of Kinetic Energy

The kinetic energy of an entire shell at the state of dynamic equilibrium is defined by

$$T^e = \frac{\rho h}{2}\iint[(\mathring{u}^e)^2 + (\mathring{v}^e)^2 + (\mathring{w}^e)^2]\, rd\theta ds \tag{55}$$

where

ρ = mass density of the shell material, and

$\mathring{u}^e, \mathring{v}^e, \mathring{w}^e$ = velocity components at the initial state of dynamic equilibrium.

Let $(\mathring{u}, \mathring{v}, \mathring{w})$ be the incremental virtual or perturbation velocity vector. Then the total velocity vector at the perturbed state is $(\mathring{u}^e+\mathring{u}, \mathring{v}^e+\mathring{v}, \mathring{w}^e+\mathring{w})$. Substituting the total velocity vector into equation (55) yields

$$T^e+\Delta T = \frac{\rho h}{2}\iint[(\mathring{u}^e+\mathring{u})^2+(\mathring{v}^e+\mathring{v})^2+(\mathring{w}^e+w)^2]\, rd\theta ds\,. \tag{56}$$

Now as before, $\Delta T = \delta T+\frac{1}{2}\delta^2 T + \ldots$, where δT is the integral of the linear terms in $(\mathring{u}, \mathring{v}, \mathring{w})$ and their derivatives, $\delta^2 T$ is the integral of the quadratic terms in $(\mathring{u}, \mathring{v}, \mathring{w})$ and their derivatives. Therefore

$$\tfrac{1}{2}\delta^2 T = \frac{\rho h}{2} \iint [\mathring{u}^2 + \mathring{v}^2 + \mathring{w}^2] \, r d\theta ds \qquad (57)$$

where

$\delta^2 T$ = second variation of kinetic energy for an entire shell.

3.6 Discrete Element Representation

3.6.1 Initial State

The shell is approximated by a system of conical frusta as shown in Figure 1. Each conical frustum is bounded by two nodal circles which are referred to hereafter as nodes. The displacements of the continuous shell are described by the displacements of these nodes. Each node has four degrees of freedom, q_1, q_2, q_3 and q_4, for asymmetric deformation as shown in Figure 3, and three degrees of freedom, q_1, q_3 and q_4, for axisymmetric deformation when torsion is excluded.

In accordance with assumption (6), p. 23, the initial displacement field within each conical shell element can be expressed by

$$\left.\begin{aligned} u^e &= \beta^e{}_5 + \beta^e{}_6 s \\ w^e &= \beta^e{}_1 + \beta^e{}_2 s + \beta^2{}_3 s^2 + \beta^e{}_4 s^3 \end{aligned}\right\} \qquad (58)$$

in which the circumferential displacement v^e is absent.

The six undetermined constants $\beta^e{}_i$ are related to the six generalized displacements $q^e{}_i$ shown in Figure 3, excluding $q_{2,p}$ and $q_{2,p+1}$, by the relation:

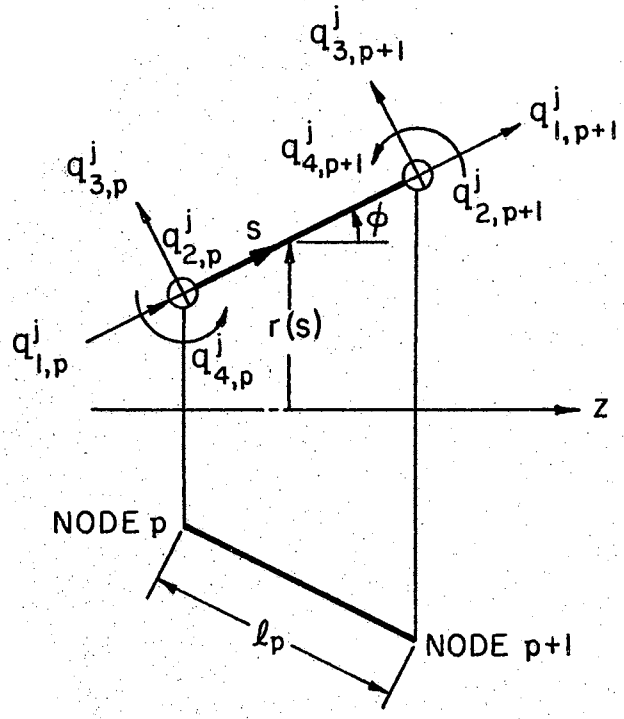

Figure 3. Generalized Coordinates

$$\{\beta^e\} = [M_e]\{q^e\} \quad . \tag{59}$$

The matrix $[M_e]$ is given in Figure 4.

By expressing the total potential energy of the continuous shell in terms of the discretized system and then using the principle of stationary total potential energy, $\delta(U^e + \Omega^e) = 0$, the equations of generalized initial forces and displacements are obtained in matrix form as

$$\sum_{p=1}^{N} ([k^e]_p\{q^e\}_p - \{Q^e\}_p) = 0 \tag{60}$$

where the summation extends over the total number of discrete elements N. The $\{q^e\}_p$ are the generalized displacements of the p^{th} discrete element and $\{Q^e\}_p$ are the corresponding generalized forces; the p^{th} discrete element is bounded by nodal stations p and p+1.

Requiring that the generalized displacements of any two adjacent elements with the same node point be the same in order to satisfy the conditions of consistent deformation, equation (60) can be written as

$$\begin{bmatrix} \\ K^e \\ \\ \end{bmatrix} \quad \begin{Bmatrix} q^e_{1,1} \\ q^e_{3,1} \\ q^e_{4,N+1} \end{Bmatrix} = \begin{Bmatrix} Q^e_{1,1} \\ Q^e_{3,1} \\ Q^e_{4,N+1} \end{Bmatrix} \tag{61}$$

$3(N+1)x3(N+1) \qquad 3(N+1)x1 \qquad 3(N+1)x1$

These equations are solved with appropriate geometric boundary conditions to obtain the equilibrium displacements $\{q^e\}$.

$$
\left[\begin{array}{c|c|c|c|c|c}
0 & 1 & 0 & 0 & 0 & 0 \\
\hline
0 & 0 & 1 & 0 & 0 & 0 \\
\hline
0 & -3/\ell_p^2 & -2/\ell_p & 0 & 3/\ell_p^2 & -1/\ell_p \\
\hline
0 & 2/\ell_p^3 & 1/\ell_p^2 & 0 & -2/\ell_p^3 & 1/\ell_p^2 \\
\hline
1 & 0 & 0 & 0 & 0 & 0 \\
\hline
-1/\ell_p & 0 & 0 & 1/\ell_p & 0 & 0
\end{array}\right]
$$

Figure 4. Matrix $[M_e]$

3.6.2 Elemental Stiffness and Stability Coefficient Matrices

The second variation of strain energy for the continuous shell $\delta^2 U$, equation (44), and the second variation of potential energy of external loads $\delta^2 \Omega$, equation (53), will be used to formulate both the elemental stiffness and stability coefficient matrices based on Donnell's theory.

First we assume that the perturbation displacements u, v and w can reasonably be approximated by the following polynomials:

$$\begin{aligned} u &= (\beta_5 + \beta_6 s)\cos j\theta \\ v &= (\beta_7 + \beta_8 s)\sin j\theta \\ w &= (\beta_1 + \beta_2 s + \beta_3 s^2 + \beta_4 s^3)\cos j\theta \ , \end{aligned} \tag{62}$$

where

$\beta_i (i=1,8)$ = undetermined constants,

j = harmonic number, or number of circumferential waves, and

s = meridional coordinates of a typical conical frustum.

The eight undetermined constants β_i are related to the eight generalized displacements q_i by the following definitions:

$$q_{1,p} = u(s)\Big|_{s=0}, q_{2,p} = v(s)\Big|_{s=0}, q_{3,p} = w(s)\Big|_{s=0}, q_{4,p} = \frac{\partial w(s)}{\partial s}\Big|_{s=0}$$

$$q_{1,p+1} = u(s)\Big|_{s=l_p}, q_{2,p+1} = v(s)\Big|_{s=l_p}, q_{3,p+1} = w(s)\Big|_{s=l_p},$$

$$q_{4,p+1} = \frac{\partial w(s)}{\partial s}\Big|_{s=l_p} \tag{63}$$

where subscript p refers to nodal station p and subscript p+1 to nodal station p+1. Thus the β's are expressed in terms of the q's by:

$$\{\beta\} = [M_p]\{q\}. \tag{64}$$

The matrix $[M_p]$ is given in Figure 5.

Recalling equations (44) and (53), the summation of both is:

$$\begin{aligned}
\tfrac{1}{2}(\delta^2 U+\delta^2\Omega) = \iint \Bigg[& \frac{C}{2}\Big\{u^2{}_{,s}+\frac{1}{r^2}(nu+v_{,\theta}+mw)^2+\frac{2\nu}{r}(nu+v_{,\theta}+mw)u_{,s} \\
& + \frac{(1-\nu)}{2r^2}(rv_{,s}+u_{,\theta}-nv)^2\Big\}+\frac{D}{2}\Big\{w^2{}_{,ss}+\left(\frac{1}{r^2}w_{,\theta\theta}+\frac{n}{r}w_{,s}\right)^2 \\
& + 2\nu\left(\frac{1}{r^2}w_{,ss}w_{,\theta\theta}+\frac{n}{r}w_{,s}w_{,ss}\right) \\
& + 2(1-\nu)\left(\frac{1}{r}w_{,s\theta}-\frac{n}{r^2}w_{,\theta}\right)^2\Big\}\Bigg] rd\theta ds \\
& + \iint\Bigg[\frac{C}{2}\Big\{2w^e{}_{,s}u_{,s}w_{,s}+u^e{}_{,s}w^2{}_{,s}+\frac{1}{r^3}(nu^e+mw^e)w^2{}_{,\theta} \\
& + \frac{\nu}{r^2}u^e{}_{,s}w^2{}_{,\theta}+\frac{\nu}{r}(nu^e+mw^e)w^2{}_{,s}+\frac{2\nu w^e{}_{,s}}{r}(nuw_{,s} \\
& + v_{,\theta}w_{,s}+mww_{,s})+\frac{(1-\nu)}{r^2}w^e{}_{,s}(rv_{,s}w_{,\theta}+u_{,\theta}w_{,\theta} \\
& - nvw_{,\theta})\Big\}\Bigg] rd\theta ds-\frac{P}{2}\iint\Big\{-uw_{,s}-\frac{1}{r}vw_{,\theta}\Big\}rd\theta ds\ . \qquad (65)
\end{aligned}$$

It will be seen that the expression $\frac{1}{2}(\delta^2 U+\delta^2\Omega)$, or equation (65), consists of three types of integrals; the integrals which do not contain initial displacements, integrals which contain initial displacements as parameters, and integrals which are the contribution of $\frac{1}{2}\delta^2\Omega$. If the displacement field, equation (62), together with the related equation (64) are substituted in equation (65)

$$
\begin{bmatrix}
0 & 0 & 1 & 0 & 0 & 0 & 0 & 0 \\
0 & 0 & 0 & 1 & 0 & 0 & 0 & 0 \\
0 & 0 & -3/\ell_p^2 & -2/\ell_p & 0 & 0 & 3/\ell_p^2 & -1/\ell_p \\
0 & 0 & 2/\ell_p^3 & 1/\ell_p^2 & 0 & 0 & -2/\ell_p^3 & 1/\ell_p^2 \\
1 & 0 & 0 & 0 & 0 & 0 & 0 & 0 \\
-1/\ell_p & 0 & 0 & 0 & 1/\ell_p & 0 & 0 & 0 \\
0 & 1 & 0 & 0 & 0 & 0 & 0 & 0 \\
0 & -1/\ell_p & 0 & 0 & 0 & 1/\ell_p & 0 & 0
\end{bmatrix}
$$

Figure 5. Matrix $[M_p]$

above, the integrals which do not contain initial displacements will yield the so called elemental stiffness matrix, and the integrals which are functions of initial displacements will yield the stability coefficient matrix. For edge-loaded shells, $\frac{1}{2}\delta^2\Omega$ is zero since Ω is a linear function of the displacements. However, for pressure-loaded shells, the $\frac{1}{2}\delta^2\Omega$ is nonzero because Ω in this case contains quadratic terms. The last integrals in equation (65) represent the contribution of $\delta^2\Omega$.

The above description is presented in the form of a matrix whose elements are functions of both elastic and geometrical properties of each frustum:

$$\frac{1}{2}(\delta^2 U+\delta^2\Omega) = \frac{1}{2}\{q\}^T\left[\iint[M_p]^T[L^j][M_p]rd\theta ds\right]\{q\} + \frac{\lambda}{2}\{q\}^T\left[\iint[M_p]^T[L^j{}_{inc}][M_p]rd\theta ds\right]\{q\} \qquad (66)$$

$$= \frac{1}{2}\{q\}^T[k]\{q\} + \frac{\lambda}{2}\{q\}^T[s]\{q\} . \qquad (67)$$

The terms in the foregoing equations are:

$[k] = \iint[M_p]^T[L^j][M_p]rd\theta ds$

= stiffness matrix of the p^{th} element in the j^{th} harmonic,

$[s] = \iint[M_p]^T[L^j{}_{inc}][M_p]rd\theta ds$

= stability coefficient matrix of the p^{th} element in the j^{th} harmonic,

$[L^j]$ = matrix contributed by the integrals in equation (65) which do not contain initial displacements,

$[L^j_{inc}]$ = matrix contributed by the integrals in equation (65) which contain initial displacements,

$[M_p]$ = transformation matrix, shown in Figure 5,

$[M_p]^T$ = transpose of matrix $[M_p]$,

$\{q\}$ = generalized perturbation displacements,

$\{q\}^T$ = transpose of matrix $\{q\}$,

λ = eigenvalue to be determined in the case of static buckling, in this work λ will be represented by hydrostatic pressure load - p, and

$r = r_p + ns$.

Furthermore

r_p = smaller radii of the p^{th} conical frustum,

$$[k] = [M_p]^T \left(\iint [L^j] r d\theta ds\right) [M_p]$$

$$= [M_p]^T [A^j] [M_p] \qquad (68)$$

and

$$[s] = [M_p]^T \left(\iint [L^j_{inc}] r d\theta ds\right) [M_p]$$

$$= [M_p]^T [B^j] [M_p] \qquad (69)$$

where

$$[A^j] = \iint [L^j] r d\theta ds$$

$$[B^j] = \iint [L^j_{inc}] r d\theta ds \, .$$

The elements of both $[A^j]$ and $[B^j]$ matrices for Donnell's theory are tabulated in Appendix B and the additional parts of both $[A^j]$ and $[B^j]$ matrices resulting from Sanders' theory are tabulated in Appendix C.

Note that for pressure-loaded shells, the contribution

of $\frac{1}{2}\delta^2\Omega$ to the stability coefficient matrix [s] in the form of matrix $[C^j]$ must be taken into account by adding it to the $[B^j]$ matrix. The matrix $[C^j]$ for both Donnell's and Sanders' theory are also tabulated in Appendices B and C, respectively.

The computation of the elements of the stability coefficient matrix requires a systematic procedure, since it depends on the initial state prior to the instability and on the type of loading.

Using equation (59), the undetermined coefficients $\{\beta^e\}$ in the assumed displacement field as given in equation (58) are given by

$$\{\beta^e\} = [M^e]\{q^e\} \tag{70}$$

where $\{q^e\}$ are the generalized initial displacements of the p^{th} element for a unit applied load. Thus, the $\{\beta^e\}$ which occur when a load P is applied becomes $P\{\beta^e\}$.

Thus we introduce

$$P\{\beta^e{}_i\} = \{G_i\} \quad (i=1,6). \tag{71}$$

For unit applied load, as an example when P is equal to 1 lb/in^2, equation (71) reduces to:

$$\{\beta^e{}_i\} = \{G_i\} \quad (i=1,6). \tag{72}$$

From equation (58), the initial displacement field becomes:

$$\begin{aligned} u^e &= G_5 + G_6 s \\ w^e &= G_1 + G_2 s + G_3 s^2 + G_4 s^3 \ . \end{aligned} \tag{73}$$

Equation (73) is the initial displacement field within which the prebuckling displacements $\{q^e\}$ of the entire structure, due to unit applied load, are contained. The substitution of this equation in the expression for $\frac{1}{2}(\delta^2 U+\delta^2\Omega)$, equation (65), yields the elements of the stability coefficient matrix in terms of G_1 to G_6 as tabulated in Appendices B and C.

3.6.3 Elemental Mass Matrix

The second variation of the kinetic energy for an entire shell at the perturbed state is

$$\frac{1}{2}\delta^2 T = \frac{\rho h}{2}\iint (\mathring{u}^2+\mathring{v}^2+\mathring{w}^2) r\,d\theta\,ds \ . \tag{74}$$

An approximation to the elemental mass matrix for the p^{th} discrete element, consistent with the approximate elemental stiffness and stability coefficient matrices, may be obtained by using the same form of the displacement function, this time with respect to velocities:

$$\begin{aligned} \mathring{u} &= (\mathring{\beta}_5 + \mathring{\beta}_6 s)\cos j\theta \\ \mathring{v} &= (\mathring{\beta}_7 + \mathring{\beta}_8 s)\sin j\theta \\ \mathring{w} &= (\mathring{\beta}_1 + \mathring{\beta}_2 s + \mathring{\beta}_3 s^2 + \mathring{\beta}_4 s^3)\cos j\theta \ . \end{aligned} \tag{75}$$

The expression (74) can be rewritten in matrix form as:

$$\begin{aligned} \frac{1}{2}\delta^2 T &= \frac{1}{2}\pi\rho h\{\mathring{q}\}^T[M_p]^T[P][M_p]\{\mathring{q}\} \\ &= \frac{1}{2}\{\mathring{q}\}^T[m]\{\mathring{q}\} \end{aligned} \tag{76}$$

where

$$[m] = \pi\rho h[M_p]^T[P][M_p]$$

[m] = elemental mass matrix for the p^{th} discrete element, and

[P] $\int_0^{l_p} r[V]ds$.

The matrix $[M_p]$ had been listed in Figure 5, whereas the matrices [V] and [P] are listed in Figure 6a and Figure 6b, respectively.

3.7 Integral $I_{\gamma\delta}$

The elements of the matrices $[A^j]$, $[B^j]$, $[C^j]$, and [m] given earlier contain variables like $I_{\gamma\delta}$ which are definite integrals of the type

$$I_{\gamma\delta} = \int_0^{l_p} r^{\gamma} s^{\delta} ds \tag{77}$$

where

$r = r_p + ns$ for conical frusta,

γ = an integer which ranges from -3 to 1, and

δ = an integer which ranges from 0 to 9.

The numerical calculation of these integrals can be approximately carried out by expanding into series with the aid of the Binomial Theorem:

$$I_{0,\delta} = \frac{l_p^{(\delta+1)}}{(\delta+1)} , \tag{78}$$

$$I_{1,\delta} = r_p \frac{l_p^{(\delta+1)}}{(\delta+1)} + n \frac{l_p^{(\delta+2)}}{(\delta+2)} , \tag{79}$$

$$I_{-1,\delta} = \frac{l_p^{(\delta+1)}}{r_p(\delta+1)} - \frac{n l_p^{(\delta+2)}}{r^2{}_p(\delta+2)} + \frac{n^2 l_p^{(\delta+3)}}{r^3{}_p(\delta+3)} - \cdots , \tag{80}$$

I	S	S^2	S^3	0	0	0	0
	S^2	S^3	S^4	0	0	0	0
		S^4	S^5	0	0	0	0
			S^6	0	0	0	0
				I	S	0	0
					S^2	0	0
SYMMETRICAL						I	S
							S^2

(a)

$I_{1,0}$	$I_{1,1}$	$I_{1,2}$	$I_{1,3}$	0	0	0	0
	$I_{1,2}$	$I_{1,3}$	$I_{1,4}$	0	0	0	0
		$I_{1,4}$	$I_{1,5}$	0	0	0	0
			$I_{1,6}$	0	0	0	0
				$I_{1,0}$	$I_{1,1}$	0	0
					$I_{1,2}$	0	0
SYMMETRICAL						$I_{1,0}$	$I_{1,1}$
							$I_{1,2}$

(b)

Figure 6. Matrices [V] and [P]

$$I_{-2,\delta} = \frac{l_p^{(\delta+1)}}{r^2{}_p(\delta+1)} - \frac{2nl_p^{(\delta+2)}}{r^3{}_p(\delta+2)} + \frac{3n^2 l_p^{(\delta+3)}}{r^4{}_p(\delta+3)} - \cdots , \quad (81)$$

$$I_{-3,\delta} = \frac{l_p^{(\delta+1)}}{r^3{}_p(\delta+1)} - \frac{3nl_p^{(\delta+2)}}{r^4{}_p(\delta+2)} + \frac{6n^2 l_p^{(\delta+3)}}{r^5{}_p(\delta+3)} - \cdots . \quad (82)$$

CHAPTER IV

PRESENTATION OF RESULTS

A computer program has been written for the IBM 360/50 electronic computer to solve equations (31), (33), and (36) for the natural frequencies, static buckling loads, and regions of dynamic instability for several truncated conical shells. The results are shown in a series of figures and tables, and are expressed non-dimensionally in terms of α, β and θ/ω for the regions of dynamic instability. As can be seen from Chapter II, the parameter α is the percentage of the static buckling load which is applied statically, β is the percentage of the static buckling load resulting from the amplitude of the pulsating load, and θ/ω is the ratio of the frequency of the pulsating load θ to the natural frequency of transverse free vibration ω of the shell. Throughout the following study, hydrostatic pulsating pressure is assumed to act on a truncated conical shell whose finite element approximation can reasonably be limited to eight in number.

An extensive study of various effects influencing the natural frequencies of free vibration, the static buckling loads, and finally the regions of dynamic instability of the shell is presented in this chapter. The various effects

investigated are:

(a) the effects of different shell theories and bending during prebuckling state,

(b) the effect of cone angle,

(c) the effect of radius to thickness ratio, and

(d) the effect of boundary conditions.

4.1 Free Vibration and Static Buckling

4.1.1 Effects of Different Shell Theories and Bending During Prebuckling State

Two types of shell theories are used for the purpose of comparing the merit of one theory to the other. The non-linear theory for thin shells developed by Sanders is applied together with Donnell's theory which is a special case of the more general and refined Sanders' theory.

Calculation is first made for free vibration of a truncated conical shell based on Donnell's theory in order to check with the available theoretical results of Seide (42) and the experimental results obtained by Weingarten (43). Therefore, the following elastic and geometrical properties are, for the time being, used:

$$E = 30 \times 10^6 \quad lb/in^2$$

$$\nu = 0.3$$

$$\text{Density} = 0.3 \quad lb/in^3$$

$$R_1 = 2.13 \quad in$$

$$R_2 = 4.866 \quad \text{in}$$

$$L = 8 \quad \text{in}$$

$$h = 0.02 \quad \text{in}$$

$$\phi = 20^{\circ}$$

The graphical representation of the above geometrical data had already been shown in Figure 2.

The calculated frequencies obtained by solving equation (31) and the corresponding experimental results (43) are shown graphically in Figure 7. The conical shells under consideration were tested with edge conditions which might be expected to approximate clamped edges, since the edges were embedded in heavy steel end plates having circular troughs filled with a low melting point alloy (42). The agreement between theory and experiment, especially for the first three modes, is reasonably good, with the experimental results falling generally below the theoretical results when the circumferential wave number is small and above the theoretical results as the wave number increases. In general, the experimental results follow the trends of the theoretical results.

Sanders' theory is next used to calculate the frequencies of vibration for the same problem, the results of which are tabulated in Table I. In Table I comparisons are made of theoretical results using Donnell's and Sanders' theory with those of Seide. Good agreement between the results of this thesis and those of Seide are observed. It is also observed that the frequencies based on Sanders'

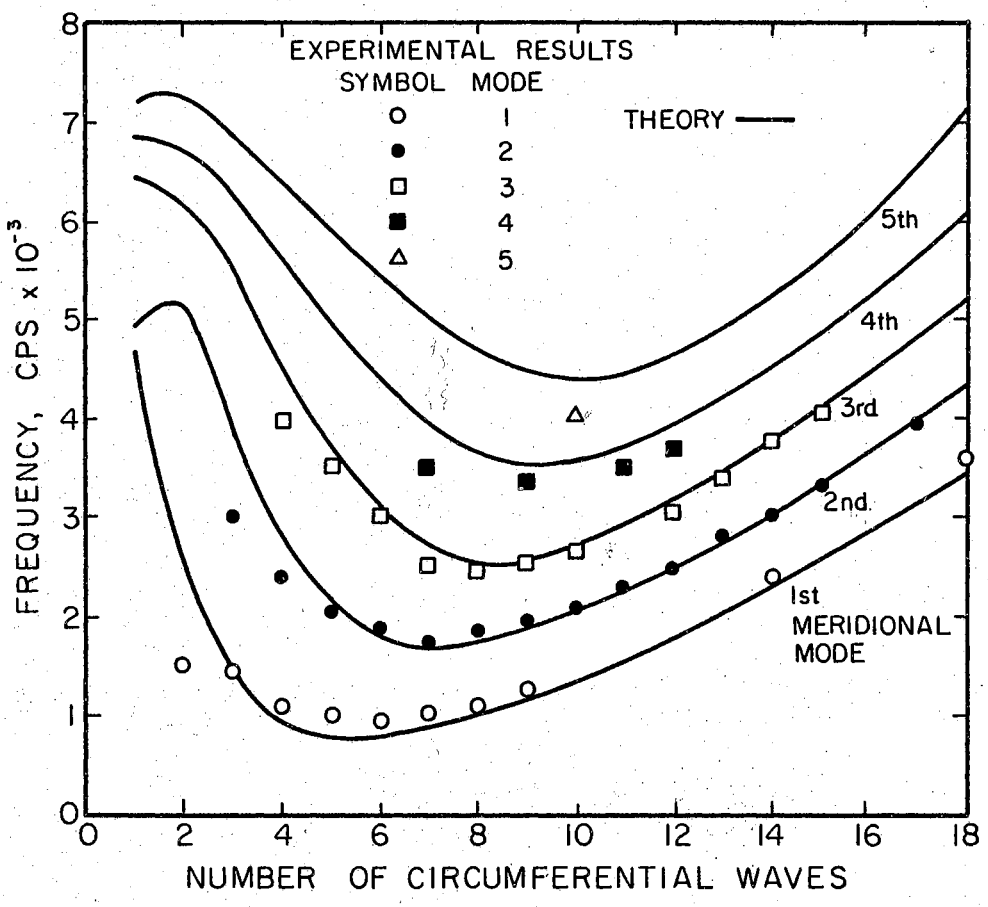

Figure 7. Comparison of the Theoretical Results From This Investigation and the Experimental Results Obtained by Weingarten (43)

TABLE I

NATURAL FREQUENCIES OF A CONICAL SHELL
SIMPLY SUPPORTED AT BOTH ENDS

$E = 30 \times 10^6$ lb/in^2	$R_1 = 2.13$ in	$L = 8$ in
Density $= 0.3$ lb/in^3	$R_2 = 4.866$ in	$h = 0.02$ in
$\nu = 0.3$	$\Phi = 20^\circ$	

i = 1

j	Donnell's Theory	Sanders' Theory	Paul Seide
2	15500	15499	16320
3	8811	8801	9100
4	5768	5741	5840
5	4672*	4620*	4692*
6	4777	4708	4780
7	5483	5413	5340
8	6382	6318	6090
9	7383	7322	7540
10	8503	8445	8350
11	9746	9690	9420
12	11110	11055	10680
13	12592	12539	11920
14	14193	14140	13500
15	15909	15857	15070
16	17741	17690	16960

*Designates the lowest eigenvalue throughout this study.

theory are always slightly lower than those based on Donnell's theory.

The static buckling loads for a shell subjected to uniform hydrostatic pressure with the same supporting condition, elastic and geometrical properties as before are obtained by solving equation (33). Both Donnell's and Sanders' theories will be applied and at the same time the consideration of a different prebuckling deformation will be carried out, i.e., the prebuckling membrane theory (PMT) and the prebuckling complete shell theory (PCT). The static buckling pressure values for the first meridional mode according to various conditions mentioned above are recorded in Table II for several circumferential wave numbers. Theoretical results of Seide (44) are also tabulated, from $j = 4, 8$, because Seide's method fails to yield reasonable buckling pressures when the circumferential wave number is small.

By Donnell's theory the lowest buckling pressure occurs at $i = 1$, $j = 6$ for both PMT and PCT and by Sanders' theory it occurs at $i = 1$, $j = 7$. Also for both PMT and PCT, the theoretical results of Seide (44) yield lowest buckling pressure at $i = 1$, $j = 6$. No matter what theories or what kind of prebuckling deformation is used, the lowest critical pressures obtained very closely agree with those of Seide. For PMT, Donnell's theory yields a lowest critical pressure about one percent lower than Seide's, whereas Sanders' theory yields a 0.2 percent higher critical pressure. It

TABLE II

BUCKLING PRESSURES FOR A SIMPLY SUPPORTED CONICAL SHELL SUBJECTED TO HYDROSTATIC PRESSURE

	i = 1				
j	Donnell's Theory		Sanders' Theory		Paul Seide
	PMT	PCT	PMT	PCT	
2	107.49	235.07	107.50	235.09	--
3	109.31	238.29	109.33	238.48	--
4	98.41	99.70	106.89	109.60	125.58
5	42.21	42.44	44.16	44.40	46.81
6	31.37*	31.53*	31.92	32.09	31.71*
7	31.51	31.68	31.77*	31.94*	32.06
8	34.00	34.26	34.20	34.45	37.63

can be concluded, for both PMT and PCT, that Donnell's theory yields a critical stress which is slightly lower than that of Seide and a more refined and general Sanders' theory yields a slightly higher one.

It has been observed that the prebuckling complete shell theory (PCT) type of deformations together with more general and exact non-linear theory for thin shells developed by Sanders can presumably yield more realistic buckling loads. The basis for such a statement has already been presented numerically in Table II and elsewhere (37), (41). Consequently, Sanders' theory with prebuckling complete shell theory will, from now on, be adopted as a reference for further investigation dealing with various effects influencing the natural frequency of free vibration, static buckling load and dynamic instability of conical shells.

4.1.2 Effect of Cone Angle

The effect of semi-vertex cone angle ϕ on free vibration and static buckling is covered in this section. It is still assumed that the structure is simply supported at both ends and the elastic and material properties remain unchanged. The only geometrical parameters changed besides cone angle are generator length L and larger radius R_2.

The natural frequencies of free vibration for semi-vertex cone angle ϕ equal to 10, 20, 30, and 45 degrees

are shown in Table III. The curves of the natural frequencies of free vibration for the first meridional and the j^{th} circumferential mode against various cone angles are depicted in Figure 8. It can be seen from Figure 8 that for a small number of circumferential waves, the natural frequencies for various cone angles are more or less close to each other. However, with increasing circumferential wave number, much difference in the natural frequencies for various cone angles is observed.

The calculated buckling pressures, as affected by the change in cone angle, are shown in Table IV and their graphical representations are depicted in Figure 9. It is seen in this figure that a high buckling pressure can be obtained with a small cone angle. However, as the cone angle increases, the allowable buckling pressure decreases. In other words, the elastic stability of the shell decreases as the cone angle of that same shell increases.

The effect of the change of cone angle on the critical buckling pressure p^* and the lowest frequency of vibration ω^* is presented graphically in Figure 10. In this particular graph one can see that the critical pressure is more sensitive to angle change than the lowest natural frequency.

A comparison between the calculated buckling pressures and those obtained through the procedure described by Kornecki (14) for various cone angles has been made and is shown in Table V. Again, good agreement between the two methods can be recognized.

TABLE III

THE NATURAL FREQUENCIES OF THE SIMPLY SUPPORTED SHELL FOR VARIOUS CONE ANGLES

$E = 30 \times 10^6$ lb/in^2 $R_1 = 2.13$ in = constant

Density = 0.3 lb/in^3 $L = 8$ in $\Phi = 10^\circ, 20^\circ, 30^\circ, 45^\circ$

$\nu = 0.3$ $h = 0.02$ in

j	$\omega_{i,j}$(rad/sec), i=1			
	$\Phi = 10^\circ$	$\Phi = 20^\circ$	$\Phi = 30^\circ$	$\Phi = 45^\circ$
2	14526.5	15498.5	15540.8	13812.6
3	8069.64	8801.05	9007.70	8284.81
4	5489.52	5741.00	5825.40	5372.43
5	5076.78*	4619.64*	4423.55	3979.31
6	5953.54	4708.31	4124.43*	3515.83*
7	7397.67	5413.37	4449.89	3597.09
8	9066.16	6317.67	5004.64	3901.27
9		7322.20		4275.05
10				4703.86
11				5191.27
12				5737.36

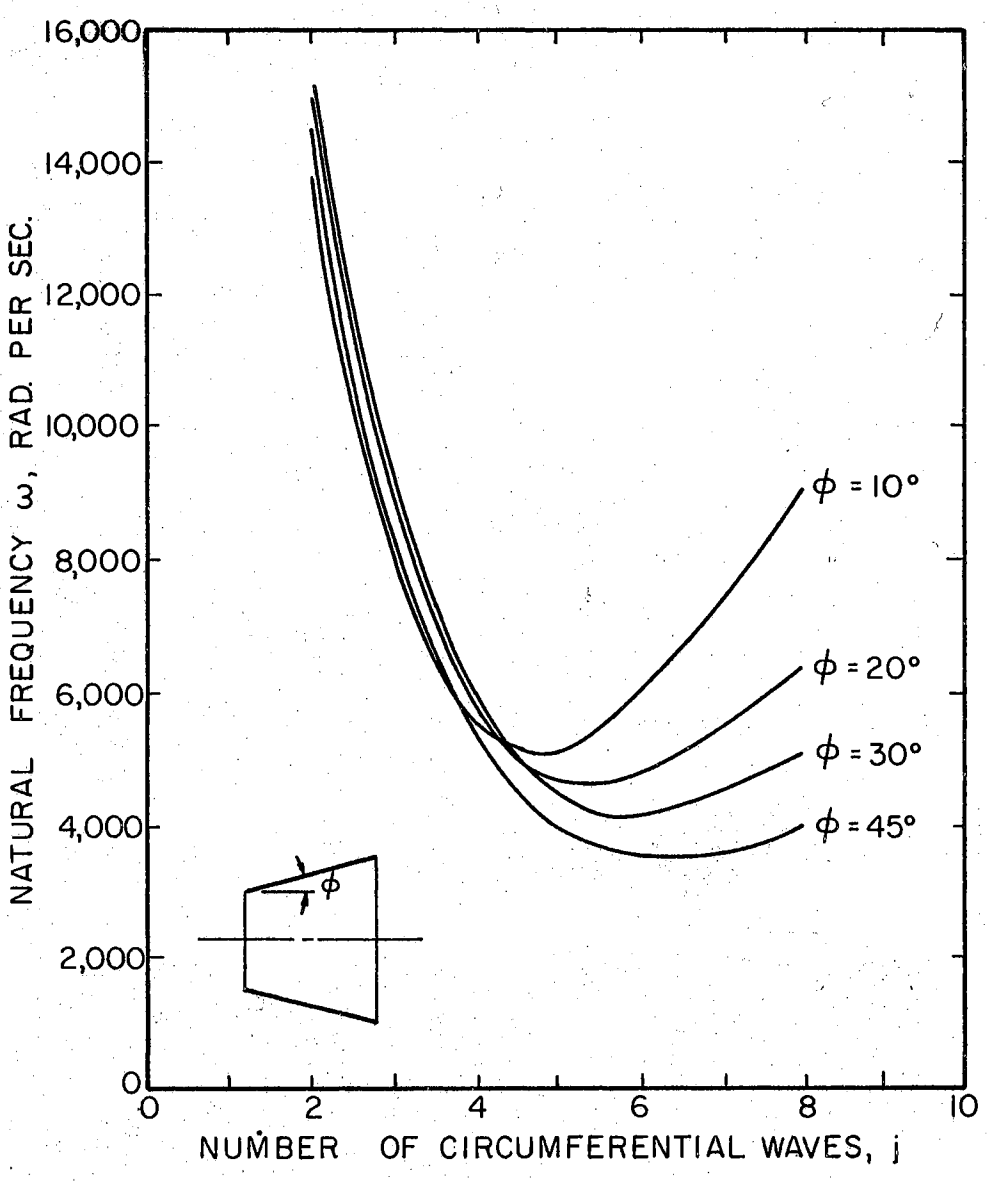

Figure 8. Comparison of the Natural Frequencies for Various Semi-Vertex Cone Angles

TABLE IV

THE BUCKLING PRESSURES OF THE SIMPLY SUPPORTED SHELL FOR VARIOUS CONE ANGLES

$E = 30 \times 10^6$ lb/in^2 $R_1 = 2.13$ in = constant

Density = 0.3 lb/in^3 L = 8 in $\Phi = 10^\circ, 20^\circ, 30^\circ, 45^\circ$

$\nu = 0.3$ h = 0.02 in

j	$p_{i,j}$(lb/in^2), i=1			
	$\Phi = 10^\circ$	$\Phi = 20^\circ$	$\Phi = 30^\circ$	$\Phi = 45^\circ$
2	407.771	235.093	153.291	85.9751
3	366.390	238.478	154.904	86.5674
4	88.5569	109.600	116.310	84.1065
5	46.9497	44.3954	42.5524	31.8281
6	44.5998*	32.0945	25.8938	17.5881
7	51.2835	31.9418*	22.7977*	14.0382
8	60.0309	34.4539	23.0179	13.2771
9		37.5940		13.1857*
10				13.4112
11				13.9047
12				14.6277

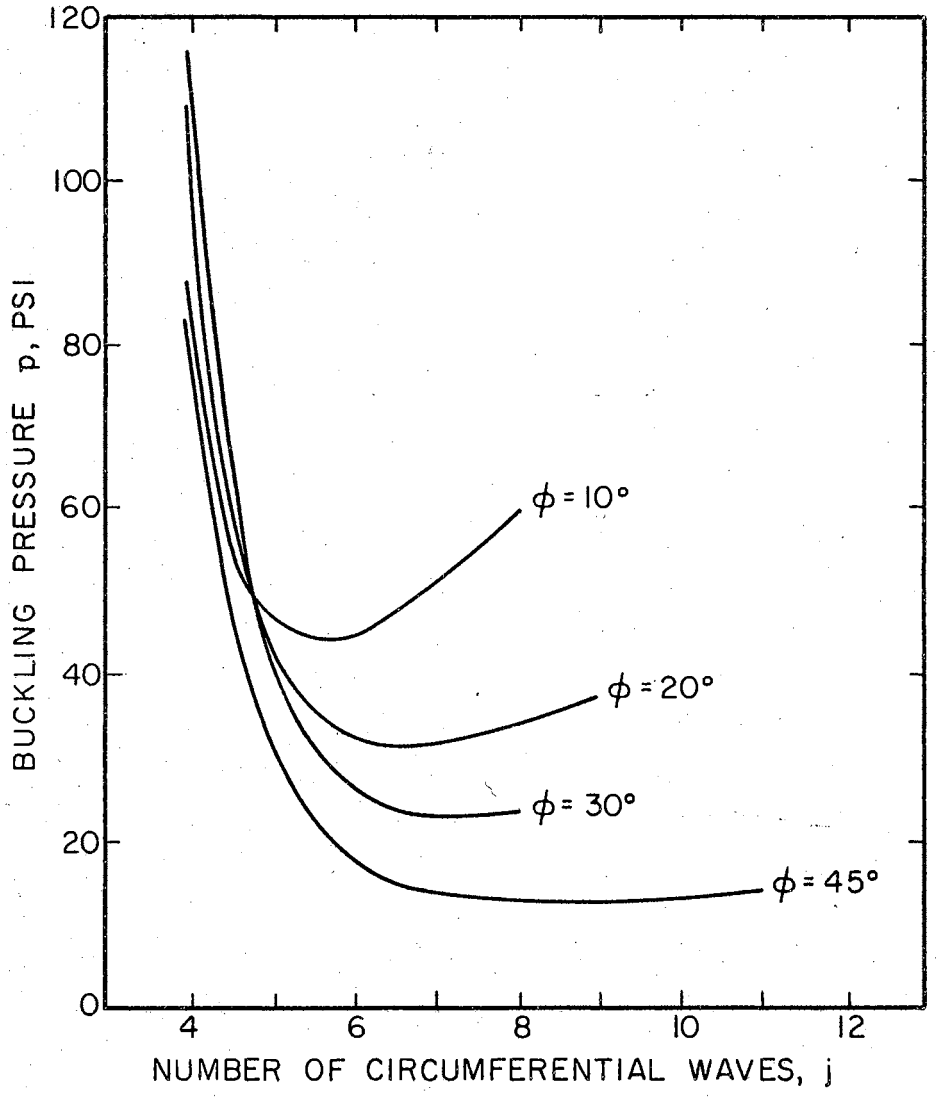

Figure 9. Comparison of the Static Buckling Pressures for Various Semi-Vertex Cone Angles

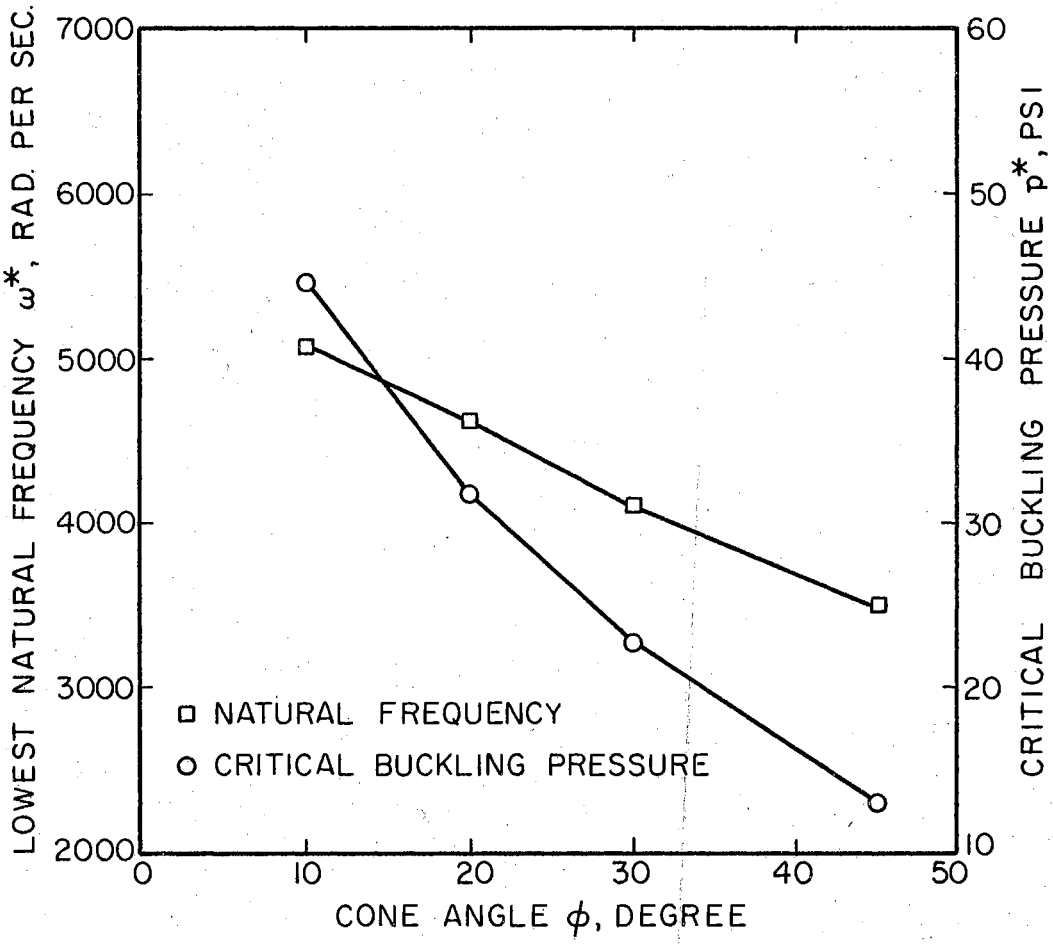

Figure 10. Effect of Cone Angle Φ on ω^* and p^* for Shell Simply Supported at Both Ends

TABLE V

BUCKLING PRESSURES OF THE SIMPLY SUPPORTED SHELL WITH VARIOUS CONE ANGLES: A COMPARISON BETWEEN THE FINITE ELEMENT METHOD (FEM) AND KORNECKI'S WORK

	$E = 30 \times 10^6$ lb/in^2		$R_1 = 2.13$ in = constant					
	Density = 0.3 lb/in^3		L = 8 in				$\Phi = 10^\circ, 20^\circ, 30^\circ, 45^\circ$	
	$\nu = 0.3$		h = 0.02 in					
	$p_{i,j}$ (lb/in^2), i=1							
j	$\Phi = 10^\circ$		$\Phi = 20^\circ$		$\Phi = 30^\circ$		$\Phi = 45^\circ$	
	FEM**	KORNECKI	FEM	KORNECKI	FEM	KORNECKI	FEM	KORNECKI
4	88.5569	88.0188	109.600	122.8671	116.310	144.9583	84.1065	122.3198
5	46.9497	45.2112	44.3954	45.7953	42.5524	48.5397	31.8281	40.2497
6	44.5998*	43.5243*	32.0945	31.0282*	25.8938	26.1887	17.5881	19.2039
7	51.2835	52.5204	31.9418*	31.3698	22.7977*	21.9139*	14.0382	13.6668
8	60.0309	65.9624	34.4539	36.8181	23.0179	23.4026	13.2771	13.0628*
9							13.1857*	14.3963
10							13.4112	16.6794

**Sanders' non-linear theory for thin shells are used.

4.1.3 Effect of Radius-Thickness Ratio

The relationship of calculated frequency to radius-thickness ratio is shown in Table VI for the ratios of 100, 240, and 500. The graphical representation of these results are depicted in Figure 11. It is assumed that the thickness h of the shell is constant and equal to 0.02 inch but the smaller radius R_1 varies (see Table VI for additional information). It can be seen from Figure 11 that, for small radius-thickness ratio, the shell natural frequencies are high and at the same time depend very strongly on the change of circumferential wave number. However, as the radius-thickness ratio increases, the natural frequencies of the shell decrease and the dependency of the frequencies on the change of wave number is somewhat decreased. It is also observed that for small radius-thickness ratios the lowest natural frequency and those which lie in its vicinity occur at small circumferential wave numbers. However, as the radius-thickness ratio increases, this set of natural frequencies occur at larger wave numbers.

The calculated buckling pressures and their graphical representations as affected by changes in radius-thickness ratio are shown in Table VII and Figure 12, respectively. Again it is seen, in Figure 12, that for small radius-thickness ratios, the shell possesses greater buckling resistivity which is, at the same time, very sensitive to the change of wave number. However, as the radius-thickness

TABLE VI

THE NATURAL FREQUENCIES OF THE SIMPLY SUPPORTED SHELL FOR VARIOUS RADIUS-THICKNESS RATIOS

$E = 30 \times 10^6$ lb/in^2 — $L = 8$ in

Density $= 0.3$ lb/in^3 — $\frac{R_1}{h} = 100, 240, 500$

$\nu = 0.3$ — $h = 0.02$ in = constant

$\Phi = 20^\circ$ — $R_1 = 2, 4.8, 10$ in

j	$\omega_{i,j}$(rad/sec), i=1		
	$\frac{R_1}{h} = 100$	$\frac{R_1}{h} = 240$	$\frac{R_1}{h} = 500$
2	15226.6	17014.0	13011.2
3	8577.12	11512.7	11033.4
4	5629.09	7962.80	8946.68
5	4663.73*	5762.94	7197.42
6	5904.13	4426.16	5821.00
7	5693.67	3683.97	4766.83
8	6643.33	3394.69*	3971.70
9	7702.58	3452.94	3381.32
10		3755.80	2958.79
11		4215.55	2680.49
12		4768.03	2525.34
13			2478.36*
14			2522.34
15			2640.61
16			2819.13

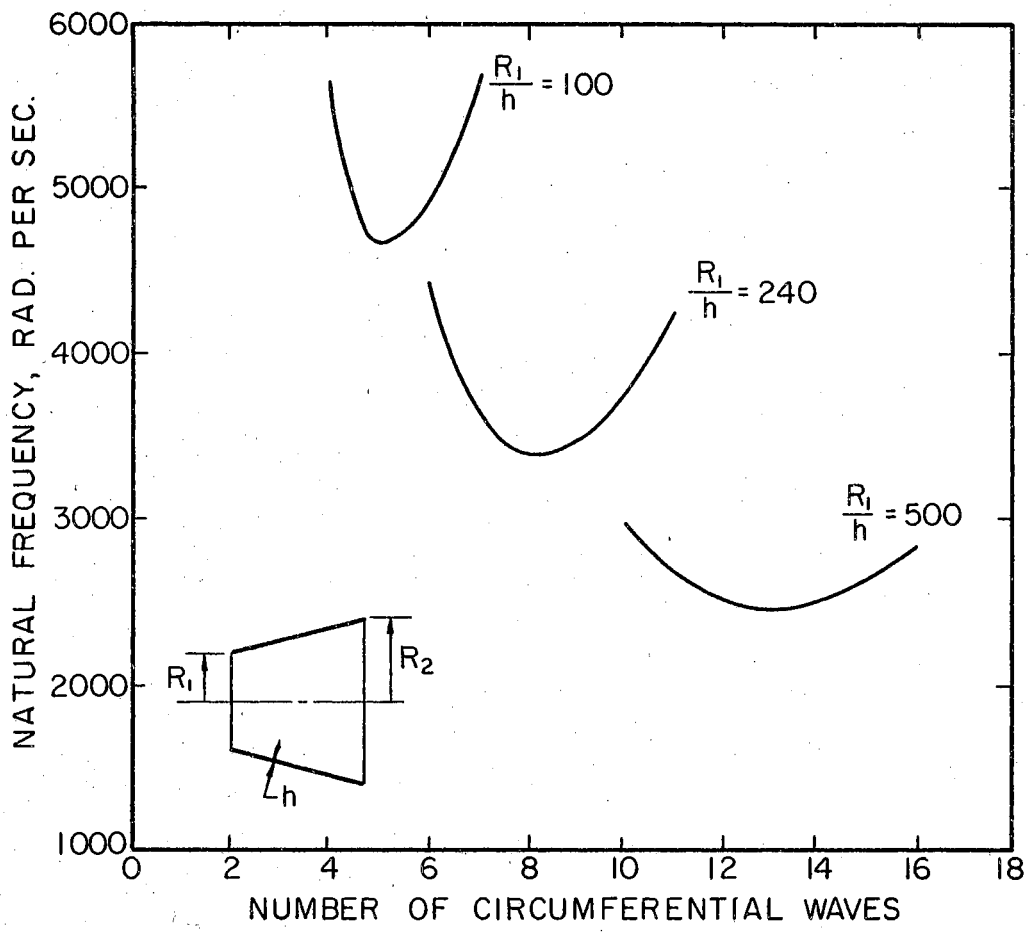

Figure 11. Effect of Radius-Thickness Ratio on Natural Frequency of Vibration

TABLE VII

THE BUCKLING PRESSURES OF THE SIMPLY SUPPORTED SHELL FOR VARIOUS RADIUS-THICKNESS RATIOS

$E = 30 \times 10^6$ lb/in^2	$L = 8$ in
Density $= 0.3$ lb/in^3	$\frac{R_1}{h} = 100, 240, 500$
$\nu = 0.3$	$h = 0.02$ in
$\Phi = 20^\circ$	$R_1 = 2, 4.8, 10$ in

j	$p_{i,j}$(lb/in^2), i=1		
	$\frac{R_1}{h} = 100$	$\frac{R_1}{h} = 240$	$\frac{R_1}{h} = 500$
2	249.562	106.042	47.9424
3	253.088	106.914	48.0850
4	101.496	107.965	48.2150
5	43.6268	109.192	48.3655
6	33.7208*	48.0203	48.5206
7	34.4084	24.5099	48.6340
8	37.1422	15.9785	36.5059
9	84.6063	13.1185	21.5255
10		12.6566*	13.5816
11		13.3066	9.32068
12		14.4812	7.01268
13			5.79524
14			5.20619
15			4.99630*
16			5.02895

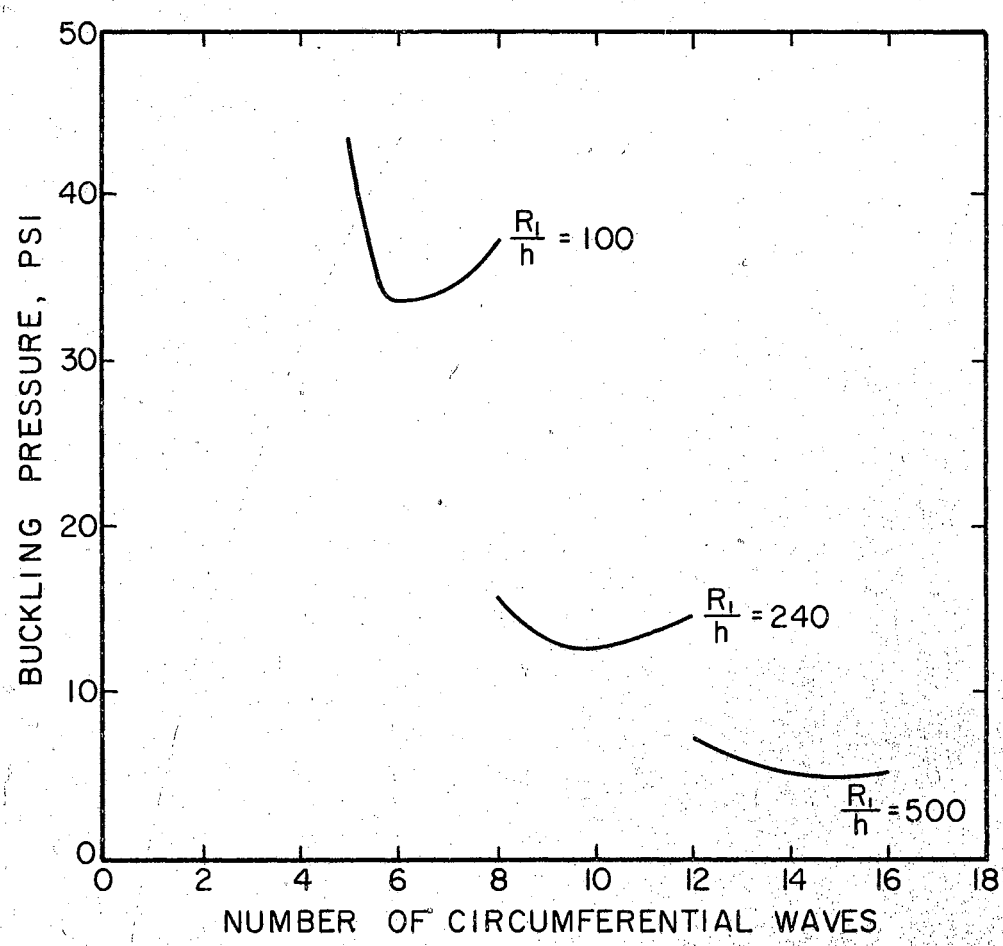

Figure 12. Effect of Radius-Thickness Ratio on Static Buckling Pressures

ratio increases, the allowable buckling pressures decrease and the influence of wave number on them also decreases.

Comparison between the calculated buckling pressures and those obtained by using the procedure described by Kornecki (14) are shown in Table VIII. A reasonably good agreement between both methods is observed.

4.1.4 Effect of Boundary Conditions

By retaining exactly the same geometrical and elastic properties of conical shells as in Section 4.1.1, the influence of boundary conditions on the natural frequencies of free vibration and buckling pressures of this structure are studied.

Three sets of boundary conditions are examined. These are listed in Table IX.

The numerical results of this investigation have been tabulated in Table X for natural frequencies of free vibration and for buckling pressures.

Since both theoretical and experimental data for the natural frequencies of vibration and buckling pressures pertaining to the above mentioned conditions are not available, no comparison can be made.

4.2 Regions of Dynamic Instability

The various effects mentioned at the beginning of this chapter which influence the dynamic stability of a truncated conical shell under the action of hydrostatic pulsating

TABLE VIII

BUCKLING PRESSURES OF SIMPLY SUPPORTED SHELL WITH VARIOUS RADIUS TO THICKNESS RATIOS: A COMPARISON BETWEEN FINITE ELEMENT METHOD AND KORNECKI'S WORK

$E = 30 \times 10^6$ lb/in^2	$\Phi = 20^o$	$\frac{R_1}{h} = 100, 240, 500$
Density $= 0.3$ lb/in^3	$L = 8$ in	$R_1 = 2, 4.8, 10$ in
$\nu = 0.3$	$h = 0.02$ in	

j	$p_{i,j}$(lb/in^2), i=1					
	$\frac{R_1}{h} = 100$		$\frac{R_1}{h} = 240$		$\frac{R_1}{h} = 500$	
	FEM**	Kornecki	FEM	Kornecki	FEM	Kornecki
4	101.496	114.0051				
5	43.6268	44.5762				
6	33.7208*	32.4133*				
7	34.4084	34.2271				
8			15.9785	15.8998		
9			13.1185	12.9194		
10			12.6566*	12.5003*		
11			13.3066	13.3149		
12					7.01268	7.0761
13					5.79524	5.8035
14					5.20619	5.1996
15					4.99630*	4.9939*
16					5.02895	5.0370

**Sanders' non-linear theory for thin shells are used.

TABLE IX

BOUNDARY CONDITIONS CONSIDERED IN THIS STUDY

TYPE	BOUNDARY CONDITIONS AT S = 0	BOUNDARY CONDITIONS AT S = L
(a)	FREE: $q_1 \neq 0, q_2 \neq 0, q_3 \neq 0, q_4 \neq 0$	FIXED: $q_{33}=q_{34}=q_{35}=q_{36}=0$
(b)	SIMPLY SUPPORTED: $q_2=q_3=0$	SIMPLY SUPPORTED: $q_{34}=q_{35}=0$
(c)	SIMPLY SUPPORTED: $q_2=q_3=0$	FIXED: $q_{33}=q_{34}=q_{35}=q_{36}=0$

TABLE X

NATURAL FREQUENCIES AND BUCKLING PRESSURES OF A TRUNCATED CONICAL SHELL UNDER VARIOUS SUPPORTING CONDITIONS

$E = 30 \times 10^6$ lb/in^2 $\quad \Phi = 20^\circ$

$\nu = 0.3$ $\quad R_1 = 2.13$ inches

Density $= 0.3$ lb/in^3 $\quad R_2 = 4.866$ inches

$L = 8$ inches $\quad h = 0.02$ inch

j	$p_{i,j}$(lb/in^2), $\omega_{i,j}$(rad/sec), i=1					
	TYPE(a)		TYPE(b)		TYPE(c)	
	$\omega_{i,j}$	$p_{i,j}$	$\omega_{i,j}$	$p_{i,j}$	$\omega_{i,j}$	$p_{i,j}$
2	10114.70	238.419	15498.50	235.093	18027.20	847.129
3	5561.69	148.381	8801.05	238.478	11664.50	815.731
4	4257.73*	46.7466	5741.00	109.600	8160.60	214.790
5	4771.38	37.6888*	4619.64*	44.3954	6446.65	83.2050
6	5751.47	42.1339	4708.31	32.0945	6044.30*	50.6017
7	6497.76	43.6582	5413.37	31.9418*	6503.32	43.9743*
8	7322.04	44.3258	6317.67	34.4539	7331.43	44.4852
9	8290.50	46.5076	7322.20	37.5940	8295.69	46.6607
10	9382.69		8445.12		9383.41	49.6593
11	10601.70		9689.98			

pressure are investigated in detail in the following sections. By solving the characteristic equation (36), the regions of dynamic instability can be plotted in a non-dimensionalized form in terms of the normalized applied loads μ (excitation parameter), and normalized frequency θ/ω. This load-frequency space will indicate whether or not a certain load applied at a given frequency will cause dynamic instability of a shell with assumed boundary conditions, elastic and geometrical properties.

4.2.1 Effects of Different Shell Theories and Bending During Prebuckling State

The dynamic stability of a truncated conical shell simply supported at both ends, whose geometrical and elastic properties are the same as those mentioned in Section 4.1.1, is examined. Again both Donnell's and Sanders' nonlinear theories for thin shells are applied. The effects of prebuckling membrane theory (PMT) and prebuckling complete shell theory (PCT) are also studied.

The necessary information for constructing the region of instability corresponding to various cases is given in Table XI. The lowest buckling pressure will be selected as a basis for computing the region of instability together with the natural frequency of free vibration whose meridional and circumferential wave numbers are the same as those for the critical buckling pressure. The regions corresponding to $\alpha = 0$ were calculated for all of the cases

TABLE XI

INFORMATION FOR CONSTRUCTING THE REGION OF INSTABILITY CORRESPONDING TO DIFFERENT SHELL THEORIES AND BENDING DURING PREBUCKLING STATE

Thin Shell Theory	Instability Boundaries					$\omega_{1,6}$ rad/sec	$p_{1,6}$ lb/in^2
	μ	$\alpha = 0$		$\alpha = 0.6$			
	0	2.0		1.2672			
Donnell	0.2	2.1897	1.7899	1.2877	1.1335		
(PMT)	0.4	2.3639	1.5510	1.4985	0.9818	4777.43	31.3677*
(I)	0.6	2.5257	1.2672	1.6016	0.8020		
Case	0.8	2.6774	0.8964	1.6985	0.5671		
Donnell	0.2	2.1900	1.7896				
(PCT)	0.4	2.3644	1.5506			4777.43	31.5344*
(II)	0.6	2.5267	1.2667				
Case	0.8	2.6788	0.8961				
Sanders'	0.2	2.1896	1.7898				
(PMT)	0.4	2.3638	1.5508			4708.31	31.9248
(III)	0.6	2.5256	1.2670				
Case	0.8	2.6773	0.8961				
	0			1.2666			
Sanders'	0.2	2.1900	1.7896	1.3870	1.1330		
(PCT)	0.4	2.3646	1.5504	1.4980	0.9812	4708.31	32.0945
(IV)	0.6	2.5268	1.2666	1.6012	0.8011		
Case	0.8	2.6791	0.8957				

*Designates lowest eigenvalue, $\mu = \frac{\beta}{2(1-\alpha)}$.

with the exception of $\alpha = 0.6$ for the first and the fourth case. It is noted that the numerical variation of each set of results is very slight. Consequently, the resulting regions of dynamic instability are almost identical for all the four cases and are therefore depicted in one figure as shown in Figure 13. It is observed that the meridional mode shape ($i = 1$) and the circumferential mode shape ($j = 6$) of the free vibration and static stability problems for all of the cases are almost identical. The pictorial representation concerning the similarity of the meridional mode shapes for free vibration and static stability is shown in Figure 14.

Table XI indicates that the effects of Donnell's and Sanders' theory for thin shells, together with PMT and PCT, on the calculated sets of results, especially for $\alpha = 0$, are very slight.

Comparison of the region of dynamic instability for $\alpha = 0.6$ using Donnell's theory (PMT) and Sanders' theory (PCT) with that of Kornecki (14) have been made for $i = 1$, $j = 6$ and the results are shown in Table XII. It should be noted that the supporting conditions, elastic and geometrical properties of the shell for both cases are identical.

Table XII shows that there is a good agreement between the calculated region of this thesis and that of Kornecki. However, it should be noted that Kornecki did his work by using Donnell's linear theory of thin shells and applied the Galerkin's method to obtain the solutions. Considering

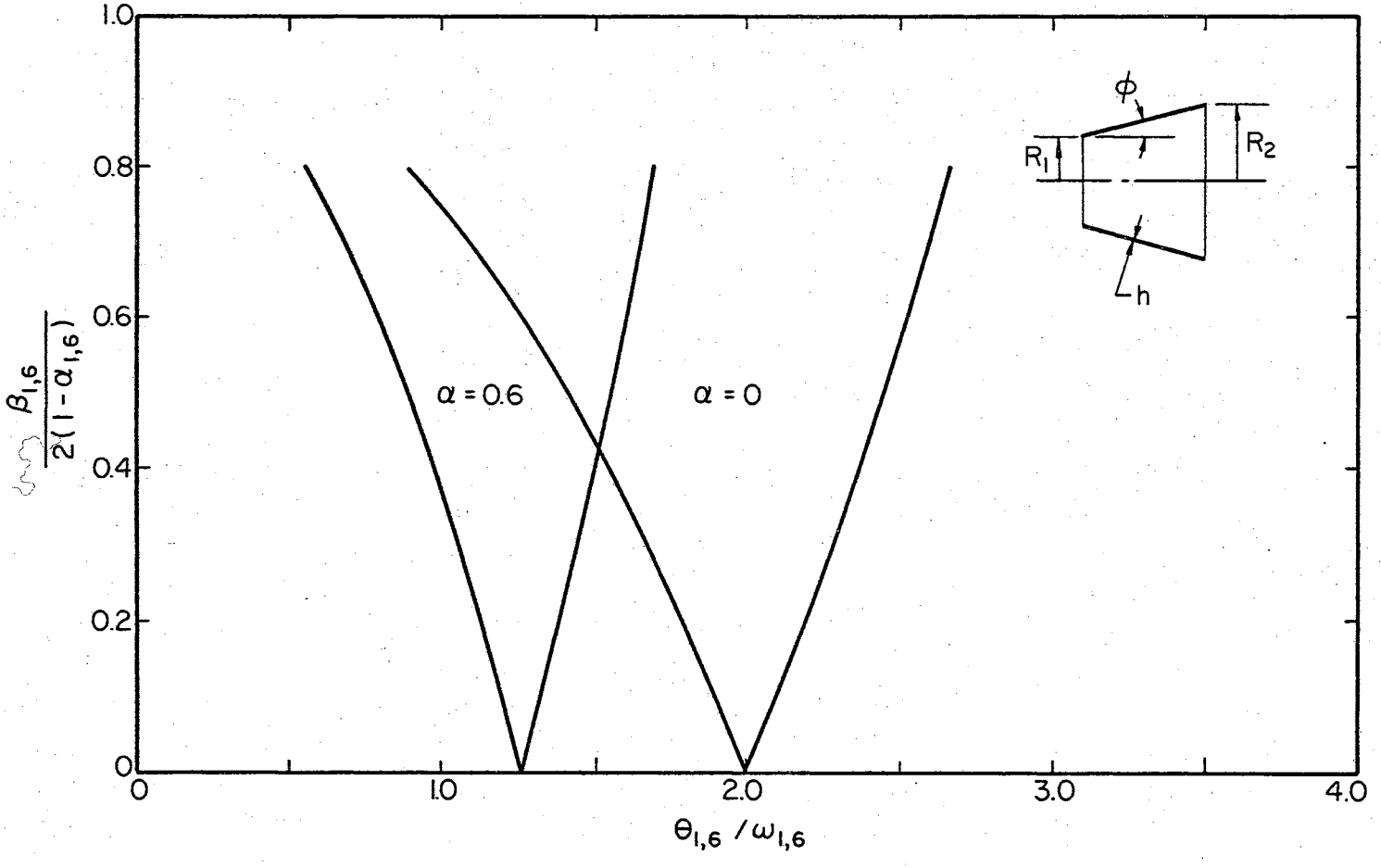

Figure 13. Regions of Dynamic Instability for a Simply Supported Shell

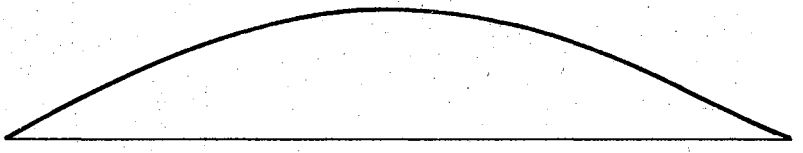

FIRST BUCKLING MODE

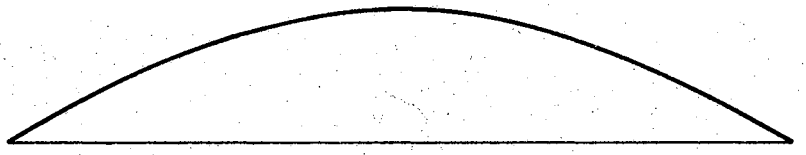

FIRST FREE VIBRATION MODE

Figure 14. Meridional Mode Shapes for a Shell Simply Supported at Both Ends

TABLE XII

COMPARISON OF INSTABILITY REGION BETWEEN THIS THESIS AND THAT OF KORNECKI

μ	INSTABILITY BOUNDARIES					
	Donnell's Theory (PMT)		Sanders' Theory (PCT)		Kornecki	
0	1.27		1.26		1.28	
0.125	1.18	1.33	1.18	1.32	1.22	1.40
0.250	1.09	1.41	1.09	1.41	1.14	1.44
0.375	1.00	1.49	1.00	1.49	1.03	1.52
0.500	0.89	1.55	0.90	1.55	0.92	1.60

the many simplifying assumptions made by Kornecki in his paper (14), and the finite element idealization in this thesis, it is difficult to assess the error involved in either works as compared to the actual regions.

In a study performed by Hutt (29), and Black (13), it was found that if the mode shapes of the structure for free vibration and static buckling are the same for equally ranked values, then the region of dynamic instability corresponding to $\alpha = 0$ is the same as the solution of the Mathieu differential equation of the form:

$$\ddot{f} + \bar{\Omega}^2(1-2\mu \cos \theta t) f = 0 \qquad (83)$$

where $f(t)$ are unknown functions of time, $\bar{\Omega}$ is the frequency of free vibrations of the structure loaded by the constant component of the time-dependent applied loads, and dot denotes differentiation with respect to time.

Since, in each of the preceding cases, the mode shapes of buckling and vibration for a given value of j were almost identical (as had been shown in Figure 14), the regions of instability are the same as those for the solutions of the Mathieu equation.

The computation of the regions of dynamic instability caused by the other effects will be carried out by using the more exact Sanders' theory with PCT, and only the region corresponding to $\alpha = 0$ is to be calculated for each case.

4.2.2 Effect of Cone Angle

The regions of instability for a simply supported conical shell whose semi-vertex angles are 10, 30 and 45 degrees are calculated and the numerical results are tabulated in Table XIII. The elastic property of the shell remains unchanged together with the smaller radius R_1 and the shell thickness h.

Again it can be seen from this table that the change of cone angle ϕ has a very slight effect on the boundary of the instability regions. The corresponding reason for this occurrence is that the mode shapes of buckling and free vibration for a given value of j are again almost identical. Their similarity was practically unaffected by the change in the semivertex angle of the cone. Therefore, according to Hutt (29), the regions of instability (for $\alpha = 0$) are the same as those for the solutions of the Mathieu equation. Since it is not practical to distinguish graphically the slight variation of numerical values between each set of results depicted in Table XIII, only one graphical presentation is shown, Figure 15.

4.2.3 Effect of Radius-Thickness Ratio

The boundaries of the region of dynamic instability for simply supported conical shell with smaller radius (R_1) to thickness (h) ratio of 100, 240 and 500 were calculated and are tabulated in Table XIV together with other necessary information. Owing to the obvious similarity between the

TABLE XIII

INFORMATION FOR CONSTRUCTING THE REGION OF INSTABILITY CORRESPONDING TO DIFFERENT CONE ANGLES

Cone Angle (degree)	Instability Boundaries			$\omega_{i,j}$ (rad/sec)	$p_{i,j}$ (lb/in^2)
	μ	$\alpha = 0$			
	0	2.0			
	0.2	2.1903	1.7893	$(\omega_{1,6})$	$(p^*_{1,6})$
10	0.4	2.3651	1.5502	5953.54	44.5998
	0.6	2.5278	1.2661		
	0.2	2.1894	1.7901	$(\omega_{1,7})$	$(p^*_{1,7})$
30	0.4	2.3633	1.5512	4449.89	22.7977
	0.6	2.5252	1.2673		
	0.2	2.1896	1.7897	$(\omega_{1,9})$	$(p^*_{1,9})$
45	0.4	2.3637	1.5511	4275.05	13.1857
	0.6	2.5253	1.2670		

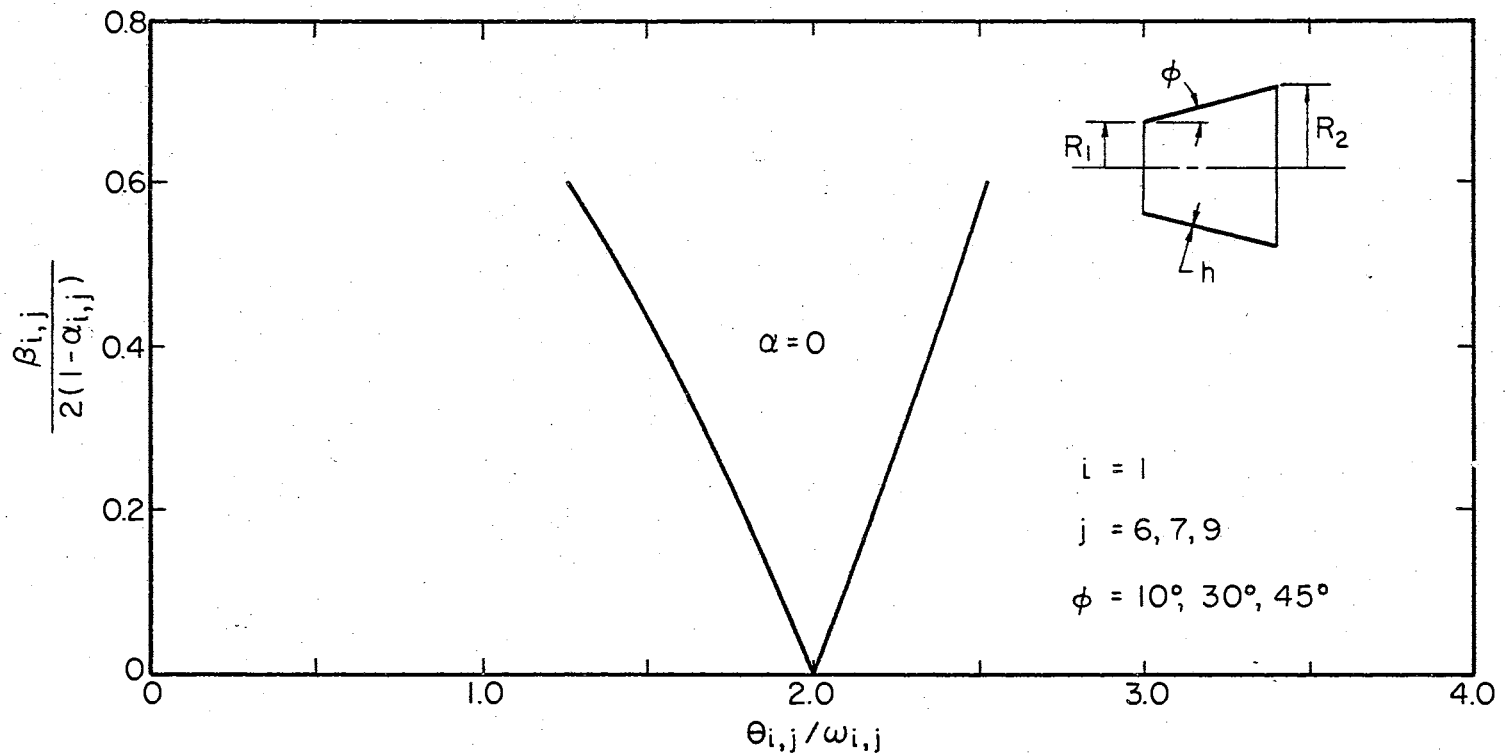

Figure 15. Region of Dynamic Instability for a Simply Supported Shell Corresponding to Different Cone Angles

TABLE XIV

INFORMATION FOR CONSTRUCTING THE REGION OF INSTABILITY CORRESPONDING TO VARIOUS RADIUS-THICKNESS RATIOS

$\frac{R_1}{h}$	Instability Boundaries			$\omega_{i,j}$ (rad/sec)	$p_{i,j}$ (lb/in^2)
	μ	$\alpha = 0$			
100	0	2.0		$(\omega_{1,6})$ 4904.13	$(p^*_{1,6})$ 33.7208
	0.2	2.1897	1.7895		
	0.4	2.3642	1.5506		
	0.6	2.5265	1.2667		
	0.8	2.6785	0.8961		
240	0.2	2.1903	1.7894	$(\omega_{1,10})$ 3755.80	$(p^*_{1,10})$ 12.6566
	0.4	2.3656	1.5500		
	0.6	2.5287	1.2660		
	0.8	2.6812	0.8957		
500	0.2	2.1907	1.7892	$(\omega_{1,15})$ 2640.61	$(p^*_{1,15})$ 4.9963
	0.4	2.3660	1.5497		
	0.6	2.5293	1.2654		
	0.8	2.6821	0.8951		

meridional mode shapes of free vibration and the static stability of the shell for a given value of j in each case, a slight variation between each set of results is expected. The graphical presentation for the three sets of results recorded in Table XIV is, therefore, shown in Figure 16. The values are observed to coincide.

4.2.4 Effect of Boundary Conditions

Three types of supporting conditions were selected to study their effect on the boundary of the region of instability. The details as to how the shell is supported are explained in Table IX. The elastic and geometrical properties of the shell are the same as those mentioned in Section 4.1.1. The numerical results for these three types of supporting conditions are tabulated in Table XV for $\alpha = 0$. Although some slight variation between each set of results corresponding to each type of supporting condition can be noticed, it is, nevertheless, quite small. Almost identical meridional mode shapes of free vibration and static buckling for each supporting condition have been observed and the sketches of these are shown in Figures 17 and 18. These are necessary for correct interpretation of the numerical results, in addition to the harmonic number j. Therefore, the region of instability corresponding to $\alpha = 0$ for each type of supporting condition was found to be almost the same as that for the solution of the Mathieu equation (29). Hence only one region of instability needs to be drawn and

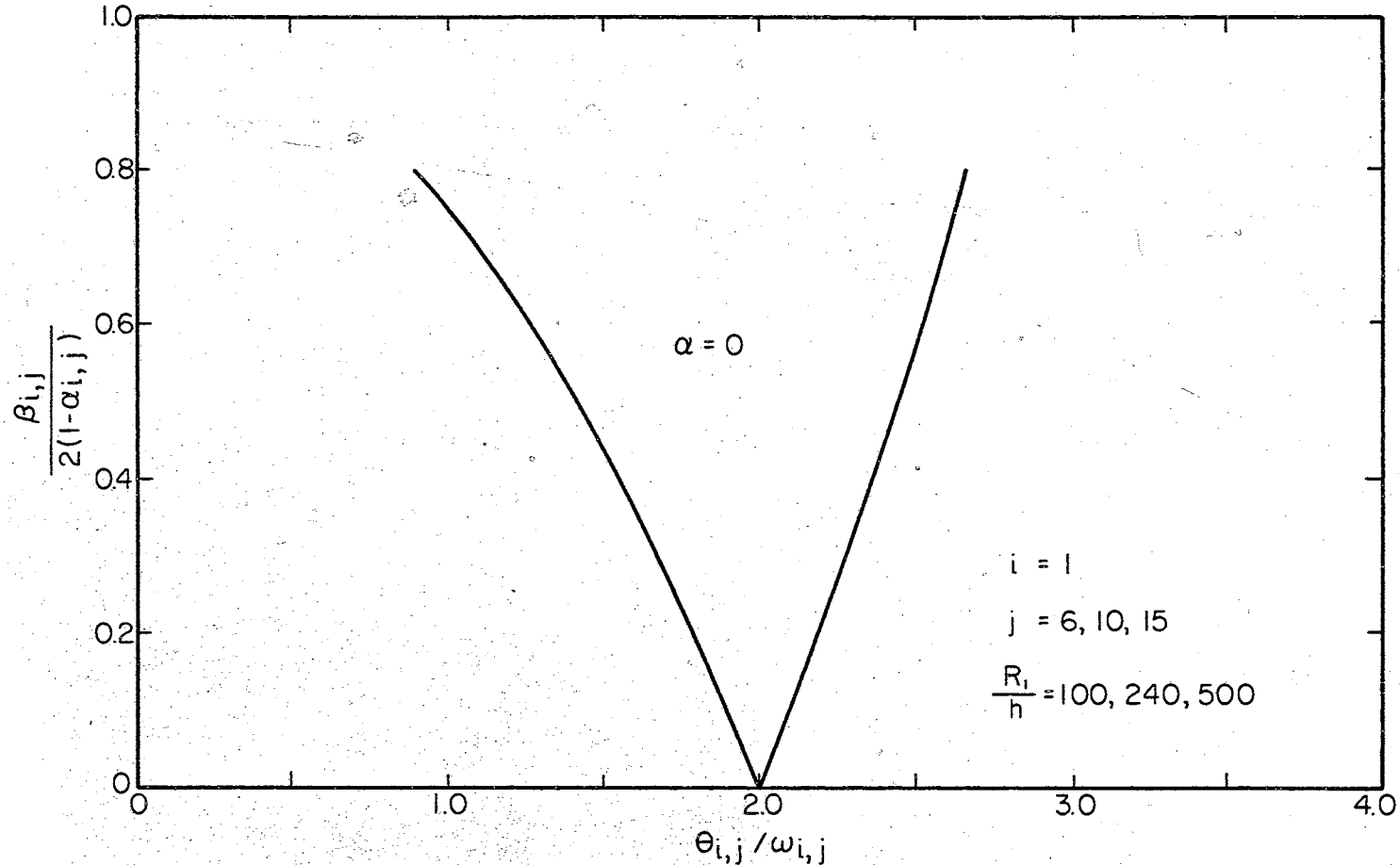

Figure 16. Region of Dynamic Instability for a Simply Supported Shell Corresponding to Various Radius-Thickness Ratio

TABLE XV

INFORMATION FOR CONSTRUCTING THE REGION OF INSTABILITY CORRESPONDING TO DIFFERENT BOUNDARY CONDITIONS

Boundary Conditions†	Instability Boundaries			$\omega_{i,j}$ (rad/sec)	$p_{i,j}$ (lb/in^2)
	μ	$\alpha = 0$			
	0	2.0			
	0.2	2.1852	1.7936		
Type (a)	0.4	2.3547	1.5576	$(\omega_{1,5})$	$(p^*_{1,5})$
(free-fixed)	0.6	2.5115	1.2754	4771.38	37.6888
	0.8	2.6579	0.9045		
	0.2	2.1900	1.7896		
Type (b)	0.4	2.3646	1.5504	$(\omega_{1,6})$	$(p_{1,6})$
(simply-simply)	0.6	2.5268	1.2666	4708.31	32.0945
	0.8	2.6791	0.8957		
	0.2	2.1888	1.7905		
Type (c)	0.4	2.3620	1.5521	$(\omega_{1,7})$	$(p^*_{1,7})$
(simply-fixed)	0.6	2.5229	1.2684	6503.32	43.9743
	0.8	2.6736	0.8977		

† See page 69 for more detailed information.

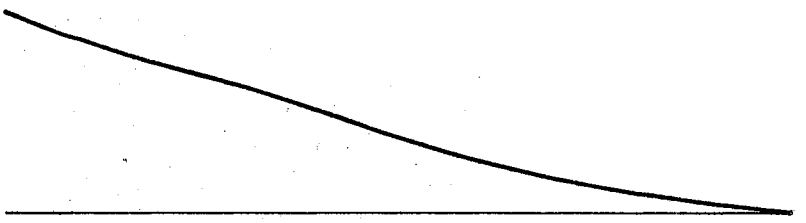

FIRST BUCKLING MODE

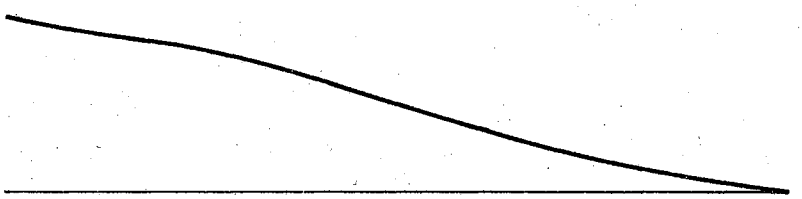

FIRST FREE VIBRATION MODE

Figure 17. Meridional Mode Shapes for a Cantilevered Shell

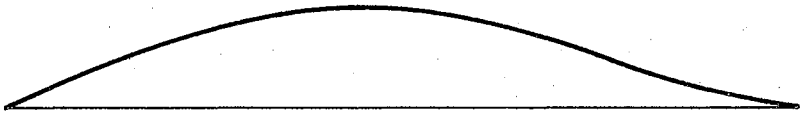

FIRST BUCKLING MODE

FIRST FREE VIBRATION MODE

Figure 18. Meridional Mode Shapes for a Shell Simply Supported at Small and Clamped at Large End

it is shown in Figure 19, since it is not practical to distinguish graphically the slight variation of numerical values between each set of results depicted in Table XV.

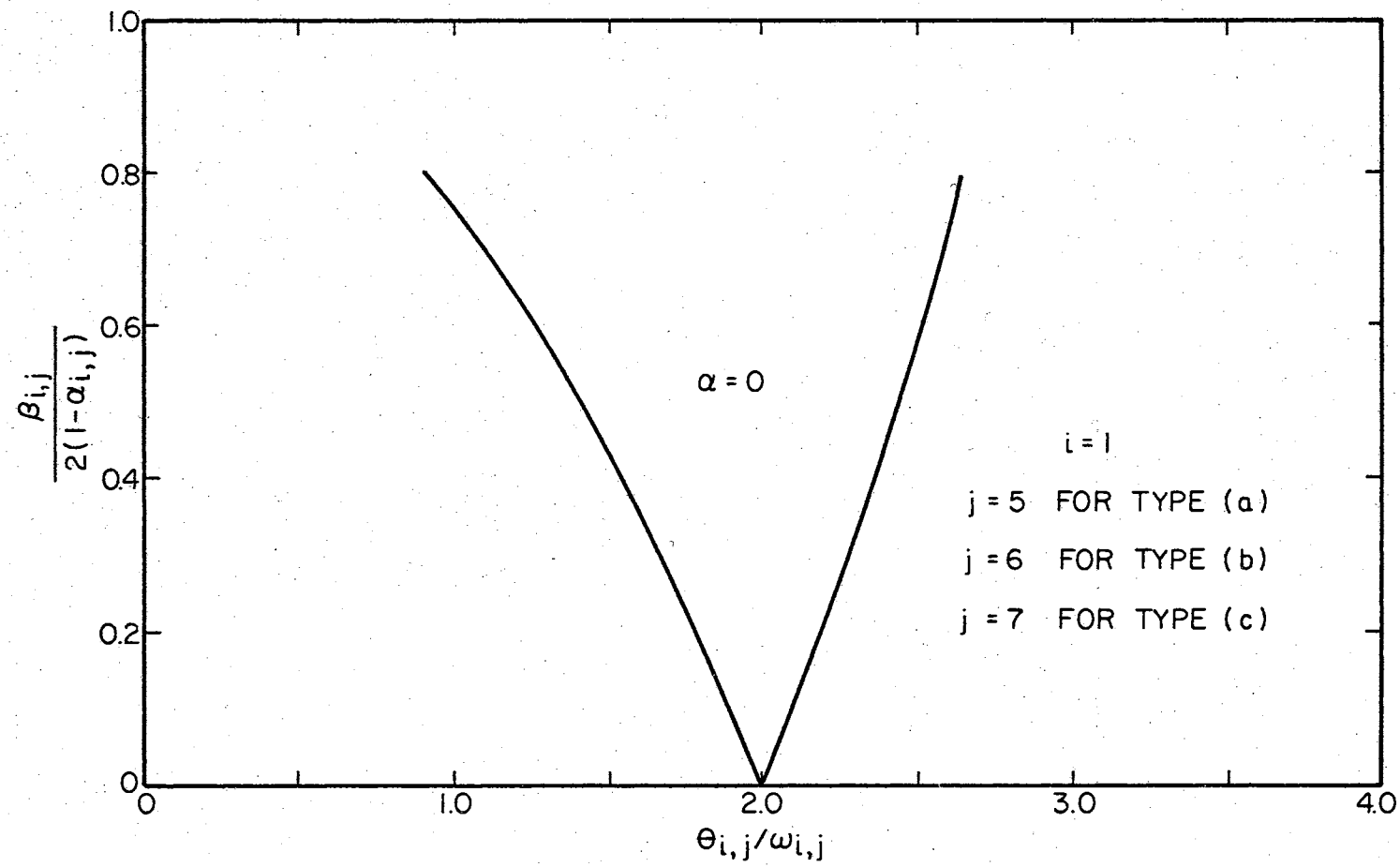

Figure 19. Region of Dynamic Instability for a Shell Under Various Supporting Conditions

CHAPTER V

SUMMARY AND CONCLUSIONS

5.1 Summary and Conclusions

A method for determining the principal regions of dynamic instability for a truncated conical shell under the action of an external uniform pulsating hydrostatic pressure has been developed in this thesis using a stiffness formulation of the finite element method. The equations of shell dynamics at equilibrium and the equations of perturbed motion of the shell were formulated from Hamilton's principle. The development of second variation expressions appearing in the equations of perturbed motion requires the consideration of geometric nonlinearity. Such nonlinearity has been introduced through the application of Sanders' nonlinear theories for thin shells. The equations of the boundaries of the regions of dynamic instability were derived from certain periodic solutions of the equations of perturbed motion. The elemental stiffness and stability coefficient matrices for any discrete element were obtained by assuming a displacement field represented by Fourier circumferential components of the generalized displacements. The accuracy of this approach was much improved by using more general and exact strain-displacement relations such as

that developed by Sanders. This approach gave natural frequencies of free vibration and static buckling loads which closely agreed with the existing theoretical and experimental data, with the use of only a few number of finite elements. The effects of different shell theories, bending during prebuckling state, cone angle, radius-thickness ratio and boundary conditions on free vibration, static buckling and dynamic instability of the shell were analyzed.

From the results presented throughout the previous chapter it is seen that, although the effects of:

(a) different shell theories and bending during prebuckling state,

(b) cone angle,

(c) radius-thickness ratio, and

(d) boundary conditions

upon the natural frequencies of free vibration ω_{ij} and static buckling loads p_{ij} of the truncated conical shell under hydrostatic pressure are very pronounced, none of these parameters seem to have a sensible influence on the overall shape of the boundaries of the principal regions of dynamic instability. It should be remembered, however, that the above cited parameters do affect the regions only in as much as they affect the scaling factors ω_{ij} and p_{ij} in Figures 13, 15, 16 and 19. The main reason behind this observation is, as explained by Hutt (29), that whenever the mode shapes for free vibration and static buckling are

identical, or nearly so, the shape of the boundaries of the instability regions will be similar to those obtained from solutions of the Mathieu-Hill equations. However, one may conceive situations where no similarity between mode shapes exist, and consequently, no similarity between the resulting regions and those of the Mathieu equation should be expected. One such case is that in which the truncated cone is acted upon by twisting couples at the ends periodically varying with time. This case was not studied in this thesis and all cases considered here yielded regions that differed in shape only slightly. This was observed to be true for virtually all cases considered, as has already been demonstrated in the preceding chapter.

The finite element method makes the study of a more complicated structures such as shell-type structures feasible. The accuracy of this method is found to be surprisingly improved if more refined nonlinear theories for thin shells are applied. Other approaches to this problem are extremely difficult unless it is simplified by unnecessary restrictions and too many questionable assumptions from the applied mechanics point of view. The effect of boundary conditions can easily be investigated by this technique, a primary advantage which has been observed. The method is very flexible in that either PMT or PCT could be used. Also, either Sanders' or Donnell's theory could be used with some modifications in the computer program employed. The finite element method, which

is based on variational principles, yields matrices that are positive definite for prebuckling equilibrium and symmetric for the perturbation problem.

5.2 Recommendations for Further Studies

The numerical examples which were solved in this thesis were confined to truncated conical shells under the action of a uniform external pulsating hydrostatic pressure. The shell is initially assumed as perfect and is made of isotropic and homogeneous material that obeys Hooke's law. The thickness of the shell is small in comparison with the radii of curvature. The method could readily be applied to other types of shells of revolution such as ellipsoidal, spherical and so on, in which the meridional curvature can be taken into account in the strain-displacement relations. The method could also be adapted to multilayer orthotropic shells. Such an extension involves no new principles provided the orthotropy is axisymmetric like the shell geometry. A logical extension of the present investigation should also include the effect of large deflections in the prebuckling equilibrium condition and the effect of initial imperfection. The dynamic stability of shells partially filled with liquid and of stiffened shells deserves special attention owing to its importance in the development of large rockets and aerospace vehicles.

BIBLIOGRAPHY

(1) Van Houten, J. J. "The Development of Sonic Environmental Testing." Institute of Environmental Sciences, Tutorial Lecture Series: Shock, Vibration and Acoustics and Education and Development, 1968, pp. 14-1, 14-11.

(2) Rayleigh, John William Strutt (Lord). The Theory of Sound. London: The Macmillan Co., Ltd., 1926.

(3) Beilin, E. A., and G. U. Dzhanelidze. "Survey of Work on the Dynamic Stability of Elastic Systems." Prikl. Mat. i Mekhan., Vol. 16, No. 5 (1952), pp. 635-648. (Available in English as ASTIA No. AD-264148.)

(4) Bolotin, V. V. Dynamic Stability of Elastic Systems. San Francisco: Holden-Day, Inc., 1964.

(5) Markov, A. N. "The Dynamic Stability of Anisotropic Cylindrical Shells." Prikl. Mat. i Mekhan., Vol. 13 (1949), pp. 145-150. (English translation, TM-43, Douglas Aircraft Company, Santa Monica, California.)

(6) Oniashvili, O. D. "On the Dynamic Stability of Shallow Shells." Soobshch. Akad. Nauk. Gruz. SSR, Vol. 9 (1950), pp. 169-175.

(7) Federhofer, Karl. "Die durch pulsierende Axialkräfte gedrückte Kreiszylindershale." Oesterr. Akad, Wiss., Math. Naturw. Kl., Vol. 163 (1954), pp. 41-54.

(8) Bolotin, V. V. "Stability of a Thin-Walled Spherical Shell Subjected to a Periodic Pressure." Collection of Papers: Design for Stability, Vol. 2, pp. 284-289, Moscow, 1958.

(9) Bublik, B. M., and V. I. Merkulov. "On the Dynamic Stability of a Thin Elastic Shell Filled with a Liquid." Prikl. Mat. i Mekhan., Vol. 24 (1960), pp. 941-947.

(10) Mettler, E. "Biegeschwingungen eines Stabes mit kleiner Vorkrümmung, exzentrisch angreifender pulsierender Axiallust und statischer Querbelastung." Forshungshefte aus d. Geb. d. Stahlbaues, Vol. 4 (1941), pp. 1-23.

(11) Naumov, K. A. "The Stability of Prismatic Rods Allowing for Damping." Tr. Mosk, Inst. Inzh. Transp., Vol. 69 (1946), pp. 132-141.

(12) Alfutov, N. A., and V. F. Razumeev. "Dynamic Stability of a Conical Shell Supported on One End and Loaded by Axisymmetric Pressure." Izvestia Akad. Nauk. SSSR, Otdel Tekhnitsheskikh Nauk., Vol. 11 (1955), pp. 161-165.

(13) Black, D. E. "Dynamic Stability of Cylindrical Shells by Finite Elements." (unpub. Ph. D. Thesis, Oklahoma State University, 1968).

(14) Kornecki, A. "Dynamic Stability of Truncated Conical Shells Under Pulsating Pressure." Israel Jour. Tech., Vol. 4, No. 1 (1966), pp. 110-120.

(15) Brachkovskii, B. Z. "On the Dynamic Stability of Elastic System." Prikl. Mat. i Mekhan. (N. S.) Vol. 6 (1942), pp. 87-88.

(16) Adini, A. "Analysis of Shell Structures by the Finite Element Method." (unpub. Ph. D. Thesis, University of California, at Berkeley, Calif., 1961).

(17) Clough, R. W., and J. L. Tocher. "Analysis of Thin Arch Dams by the Finite Element Method." Proceedings of the International Symposium on the Theory of Arch Dams, Southampton University, England, 1964.

(18) Zienkiewicz, O. C., and Y. Cheung. "Finite Element Method of Analysis for Arch Dams and Comparison with Finite Difference Procedures." Proceedings of the International Symposium on the Theory of Arch Dams, Southampton University, England, 1964.

(19) Grafton, P. E., and D. R. Strome. "Analysis of Axisymmetric Shells by the Direct Stiffness Method." AIAA Journal, Vol. 1, No. 10 (1963), pp. 2342-2347.

(20) Percy, J. H., T. H. H. Pian, S. Klein, and D. R. Navaratna. "Application of Matrix Displacement Method to Linear Elastic Analysis of Shells of Revolution." AIAA Journal, Vol. 3, No. 11 (1965), pp. 2138-2145.

(21) Dong, S. B. "Analysis of Laminated Shells of Revolution." Journal of Engineering Mechanics Division, ASCE, Vol. 92, EM6, Proc. Paper 5044 (1966), pp. 135-155.

(22) Navaratna, D. R. "Computation of Stress Resultants in Finite Element Analysis." AIAA Journal, Vol. 4, No. 11 (1966), pp. 2058-2060.

(23) Jones, R. E., and D. R. Strome. "Direct Stiffness Method Analysis of Shells of Revolution Utilizing Curved Elements." AIAA Journal, Vol. 4, No. 9 (1966), pp. 1519-1525.

(24) Stricklin, J. A., D. R. Navaratna, and T. H. H. Pian. "Improvements on the Analysis of Shells of Revolution by the Matrix Displacement Method." AIAA Journal, Vol. 4, No. 11 (1966), pp. 2069-2072.

(25) Utku, S. "Stiffness Matrices for Thin Triangular Elements of Nonzero Gaussian Curvature." Presented at the 4th Aerospace Sciences Meeting, Los Angeles, Calif., 1966.

(26) Webster, J. J. "Free Vibrations of Shells of Revolution Using Ring Finite Elements." Int. J. Mech. Sci., Vol. 9 (1967), pp. 559-570.

(27) Connor, J. J., and C. Brebbia. "Stiffness Matrix for Shallow Rectangular Shell Element." Journal of the Engineering Mechanics Division, ASCE, Vol. 93, EM5 (1967), pp. 43-65.

(28) Brown, J. E. "Dynamic Stability of Bars by the Finite Element Method." (unpub. Master's Report, Oklahoma State University, 1968).

(29) Hutt, J. M. "Dynamic Stability of Plates by Finite Elements." (unpub. Ph. D. Thesis, Oklahoma State University, 1968).

(30) Turner, M. J., et al. "Large Deflections of Structures Subjected to Heating and External Loads." Jour. Aero. Sciences, Vol. 27 (1960), pp. 97-101.

(31) Archer, J. S. "Consistent Matrix Formulation for Structural Analysis Using Influence Coefficient Techniques." AIAA Journal, Vol. 3, No. 10 (1965), pp. 1910-1918.

(32) Gallagher, R. H., et al. "A Discrete Element Procedure for Thin-Shell Instability Analysis." AIAA Journal, Vol. 5, No. 1 (1967), pp. 138-165.

(33) Argyris, J. H. "Recent Advances in Matrix Methods of Structural Analysis." Progress in Aeronautical Sciences, Vol. 4, Pergamon Press, New York, 1964.

(34) Martin, H. C. "On the Derivation of Stiffness Matrices for the Analysis of Large Deflection and Stability Problems." Proceedings of the Conference on Matrix Methods in Structural Mechanics, Wright Patterson AFB, Ohio (1966), pp. 697-716.

(35) Kapur, K. K., and B. J. Hartz. "Stability of Plates Using the Finite Element Method." Journal of the Engineering Mechanics Division, ASCE, Vol. 92 (1966), pp. 177-195.

(36) Oden, J. T. "Calculation of Geometric Stiffness Matrices for Complex Structures." AIAA Journal, Vol. 4, No. 8 (1966), pp. 1480-1482.

(37) Navaratna, D. R. "Elastic Stability of Shells of Revolution by the Variational Approach Using Discrete Elements." (unpub. Sc. D. Thesis, MIT, Department of Aeronautics and Astronautics, Cambridge, Mass., 1966).

(38) Langhaar, H. L. Energy Methods in Applied Mechanics. New York: John Wiley and Sons, Inc., 1962.

(39) Nowacki, W. Dynamics of Elastic Systems. New York: John Wiley and Sons, Inc., 1963.

(40) Vijayaraghavan, A., and R. M. Evan-Iwanowski. "Parametric Instability of Cylindrical Shells." Proceedings of the Fifth U. S. National Congress of Applied Mechanics, 1966, pp. 174.

(41) Sanders, J. L., Jr. "Nonlinear Theories for Thin Shells." Quar. App. Math., Vol. 21, No. 1 (1963), pp. 21-36.

(42) Seide, P. "On the Free Vibrations of Simply Supported Truncated Conical Shells." Israel Jour. Tech., Vol. 3, No. 1 (1965), pp. 50-61.

(43) Weingarten, V. I. "Experimental Investigation of the Free Vibration of Multi-Layed Cylindrical Shells." Aerospace Corporation Report TDR-69 (2240-65) TR-2.

(44) Seide, P. "On the Buckling of Truncated Conical Shells Under Uniform Hydrostatic Pressure." Proc. Symp. on the Theory of Thin Elastic Shells, Ed. W. T. Koiter. Amsterdam: North Holland Publishing Co., 1960, pp. 363-388.

APPENDIX A

SANDERS' STRAIN-DISPLACEMENT RELATIONS

In the formulation of the elemental stiffness and stability coefficient matrices of this thesis, Sanders' strain-displacement relations are used. They are

$$
\begin{aligned}
\epsilon_s &= (u,_s - w\Phi,_s) + \tfrac{1}{2}(\Psi^2{}_s + \Psi^{*2}) \\
\epsilon_\theta &= (1/r)(u \sin\Phi + v,_\theta + w\cos\Phi) + \tfrac{1}{2}(\Psi^2{}_\theta + \Psi^{*2}) \\
\epsilon_{s\theta} &= (1/2r)(rv,_s + u,_\theta - v\sin\Phi) + \tfrac{1}{2}\Psi_s\Psi_\theta \\
\kappa_s &= \Psi_{s,s} \\
\kappa_\theta &= (1/r)(\Psi_{\theta,\theta} + \Psi_s \sin\Phi) \\
\kappa_{s\theta} &= \tfrac{1}{2}\left[\Psi_{\theta,s} + \frac{1}{r}\Psi_{s,\theta} - \Psi_\theta \frac{\sin\Phi}{r} + \left(\Phi,_s + \frac{\cos\Phi}{r}\right)\Psi^*\right]
\end{aligned}
\tag{A1}
$$

where

$$
\begin{aligned}
\Psi_s &= -(w,_s + u\Phi,_s) \\
\Psi_\theta &= -(1/r)(w,_\theta - v\cos\Phi^*) \\
\Psi^* &= (1/2r)(rv,_s + v\sin\Phi - u,_\theta)
\end{aligned}
$$

$u,_s \equiv \frac{\partial u}{\partial s}$ $\Phi,_s \equiv \frac{\partial \Phi}{\partial s}$ etc.

Φ = meridional shape for each element

= constant for conical shells

The strain-displacement relations for Donnell's theory are obtained from equation (A1) by dropping terms with the asterisk. The strains and curvature changes for the e state, denoted by $\epsilon^e_{\alpha\beta}$ and $\kappa^e_{\alpha\beta}$ are obtained by taking only the

linear parts of equation (A1). Since the meridional shape Φ for any typical conical frustum does not vary with the meridional distance s, the partial derivative of Φ with respect to s is equal to zero.

APPENDIX B

THE $[A^j]$, $[B^j]$, AND $[C^j]$ MATRICES FROM DONNELL'S THEORY

$[A^j]$ Matrix

$$A^j_{1,1} = \pi\{Cm^2 I_{-1,0} + D[j^4 + 2(1-\nu)n^2 j^2] I_{-3,0}\}$$

$$A^j_{1,2} = \pi\{Cm^2 I_{-1,1} - D[(3-2\nu)nj^2] I_{-2,0} + D[j^4 + 2(1-\nu)n^2 j^2] I_{-3,1}\}$$

$$A^j_{1,3} = \pi\{Cm^2 I_{-1,2} - 2D\nu j^2 I_{-1,0} - 2D[(3-2\nu)nj^2] I_{-2,1} + D[j^4 + 2(1-\nu)n^2 j^2] I_{-3,2}\}$$

$$A^j_{1,4} = \pi\{Cm^2 I_{-1,3} - 6D\nu j^2 I_{-1,1} - 3D[(3-2\nu)nj^2] I_{-2,2} + D[j^4 + 2(1-\nu)n^2 j^2] I_{-3,3}\}$$

$$A^j_{1,5} = \pi Cmn I_{-1,0}$$

$$A^j_{1,6} = \pi\{Cmn I_{-1,1} + C\nu m I_{0,0}\}$$

$$A^j_{1,7} = \pi Cmj I_{-1,0}$$

$$A^j_{1,8} = \pi Cmj I_{-1,1}$$

$$A^j_{2,2} = \pi\{Cm^2 I_{-1,2} + D[n^2 + 2(1-\nu)j^2] I_{-1,0} - 2D[(3-2\nu)nj^2] I_{-2,1} + D[j^4 + 2(1-\nu)n^2 j^2] I_{-3,2}\}$$

$$A^j_{2,3} = \pi\{Cm^2 I_{-1,3}+2D\nu nI_{0,0}+2D[n^2+(2-3\nu)j^2]I_{-1,1} - 3D[(3-2\nu)nj^2]I_{-2,2}+D[j^4+2(1-\nu)n^2j^2]I_{-3,3}\}$$

$$A^j_{2,4} = \pi\{Cm^2 I_{-1,4}+6D\nu nI_{0,1}+3D[n^2+(2-4\nu)j^2]I_{-1,2} - 4D[(3-2\nu)nj^2]I_{-2,3}+D[j^4+2(1-\nu)n^2j^2]I_{-3,4}\}$$

$$A^j_{2,5} = \pi Cmn I_{-1,1}$$

$$A^j_{2,6} = \pi\{Cmn I_{-1,2}+C\nu m I_{0,1}\}$$

$$A^j_{2,7} = \pi Cmj I_{-1,1}$$

$$A^j_{2,8} = \pi Cmj I_{-1,2}$$

$$A^j_{3,3} = \pi\{Cm^2 I_{-1,4}+4DI_{1,0}+8D\nu nI_{0,1}+4D[n^2+(2-3\nu)j^2]I_{-1,2} - 4D[(3-2\nu)nj^2]I_{-2,3}+D[j^4+2(1-\nu)n^2j^2]I_{-3,4}\}$$

$$A^j_{3,4} = \pi\{Cm^2 I_{-1,5}+12DI_{1,1}+18D\nu nI_{0,2}+6D[n^2+2-\tfrac{10}{3}\nu j^2]I_{-1,3} - 5D[(3-2\nu)nj^2]I_{-2,4}+D[j^4+2(1-\nu)n^2j^2]I_{-3,5}\}$$

$$A^j_{3,5} = \pi Cmn I_{-1,2}$$

$$A^j_{3,6} = \pi\{Cmn I_{-1,3}+C\nu m I_{0,2}\}$$

$$A^j_{3,7} = \pi Cmj I_{-1,2}$$

$$A^j_{3,8} = \pi Cmj I_{-1,3}$$

$$A^j_{4,4} = \pi\{Cm^2 I_{-1,6}+36DI_{1,2}+36D\nu nI_{0,3}+3D[3n^2+(6-10\nu)j^2]I_{-1,4} - 6D[(3-2\nu)nj^2]I_{-2,5}+D[j^4+2(1-\nu)n^2j^2]I_{-3,6}\}$$

$$A^j_{4,5} = \pi Cmn I_{-1,3}$$

$$A^j_{4,6} = \pi\{Cmn I_{-1,4} + C\nu n I_{0,3}\}$$

$$A^j_{4,7} = \pi Cmj I_{-1,3}$$

$$A^j_{4,8} = \pi Cmj I_{-1,4}$$

$$A^j_{5,5} = \pi C\left[n^2 + \frac{(1-\nu)}{2} j^2\right] I_{-1,0}$$

$$A^j_{5,6} = \pi\{C\left[n^2 + \frac{(1-\nu)}{2} j^2\right] I_{-1,1} + C\nu n I_{0,0}\}$$

$$A^j_{5,7} = \pi C\left[\frac{(3-\nu)}{2} nj\right] I_{-1,0}$$

$$A^j_{5,8} = \pi\{C\left[\frac{(3-\nu)}{2} nj\right] I_{-1,1} - C\frac{(1-\nu)}{2} j I_{0,0}\}$$

$$A^j_{6,6} = \pi\{CI_{1,0} + 2C\nu n I_{0,1} + C\left[n^2 + \frac{(1-\nu)}{2} j^2\right] I_{-1,2}\}$$

$$A^j_{6,7} = \pi\{C\nu j I_{0,0} + C\left[\frac{(3-\nu)}{2} nj\right] I_{-1,1}\}$$

$$A^j_{6,8} = \pi\{C\left[\frac{(3\nu-1)}{2} j\right] I_{0,1} + C\left[\frac{(3-\nu)}{2} nj\right] I_{-1,2}\}$$

$$A^j_{7,7} = \pi C\left[j^2 + \frac{(1-\nu)}{2} n^2\right] I_{-1,0}$$

$$A^j_{7,8} = \pi\{-C\frac{(1-\nu)}{2} n I_{0,0} + C\left[j^2 + \frac{(1-\nu)}{2} n^2\right] I_{-1,1}\}$$

$$A^j_{8,8} = \pi\{C\frac{(1-\nu)}{2} I_{1,0} + C\left[j^2 + \frac{(1-\nu)}{2} n^2\right] I_{-1,2} - C(1-\nu) n I_{0,1}\}$$

The elements of $[A^o]$ are obtained from the above elements by substituting $j = 0$ and by replacing π by 2π.

[B^j] Matrix

$$B^j_{1,1} = \pi C\{j^2(mG_1I_{-2,0}+mG_2I_{-2,1}+mG_3I_{-2,2}+mG_4I_{-2,3}+nG_5I_{-2,0} + nG_6I_{-2,1})+\nu j^2G_6I_{-1,0}\}$$

$$B^j_{1,2} = \pi C\{j^2(mG_1I_{-2,1}+mG_2I_{-2,2}+mG_3I_{-2,3}+mG_4I_{-2,4}+nG_5I_{-2,1} + nG_6I_{-2,2})+\nu j^2G_6I_{-1,1}+\nu m(G_2I_{0,0}+2G_3I_{0,1}+3G_4I_{0,2})\}$$

$$B^j_{1,3} = \pi C\{j^2(mG_1I_{-2,2}+mG_2I_{-2,3}+mG_3I_{-2,4}+mG_4I_{-2,5}+nG_5I_{-2,2} + nG_6I_{-2,3})+\nu j^2G_6I_{-1,2}+2\nu m(G_2I_{0,1}+2G_3I_{0,2} + 3G_4I_{0,3})\}$$

$$B^j_{1,4} = \pi C\{j^2(mG_1I_{-2,3}+mG_2I_{-2,4}+mG_3I_{-2,5}+mG_4I_{-2,6}+nG_5I_{-2,3} + nG_6I_{-2,4})+\nu j^2G_6I_{-1,3}+3\nu m(G_2I_{0,2}+2G_3I_{0,3} + 3G_4I_{0,4})\}$$

$$B^j_{1,5} = \pi C\{\frac{(1-\nu)}{2} j^2(G_2I_{-1,0}+2G_3I_{-1,1}+3G_4I_{-1,2})\}$$

$$B^j_{1,6} = \pi C\{\frac{(1-\nu)}{2} j^2(G_2I_{-1,1}+2G_3I_{-1,2}+3G_4I_{-1,3})\}$$

$$B^j_{1,7} = \pi C\{\frac{(1-\nu)}{2} nj(G_2I_{-1,0}+2G_3I_{-1,1}+3G_4I_{-1,2})\}$$

$$B^j_{1,8} = \pi C\{-\frac{(1-\nu)}{2} j(G_2I_{0,0}+2G_3I_{0,1}+3G_4I_{0,2}) + \frac{(1-\nu)}{2}nj(G_2I_{-1,1} + 2G_3I_{-1,2}+3G_4I_{-1,3})\}$$

$$B^j_{2,2} = \pi C\{G_6I_{1,0}+j^2(mG_1I_{-2,2}+mG_2I_{-2,3}+mG_3I_{-2,4}+mG_4I_{-2,5} + nG_5I_{-2,2}+nG_6I_{-2,3})+\nu j^2G_6I_{-1,2}+\nu(mG_1I_{0,0}+mG_2I_{0,1} + mG_3I_{0,2}+mG_4I_{0,3}+nG_5I_{0,0}+nG_6I_{0,1})+2\nu m(G_2I_{0,1} + 2G_3I_{0,2}+3G_4I_{0,3})\}$$

$$B^j_{2,3} = \pi C\{2G_6I_{1,1}+j^2(mG_1I_{-2,3}+mG_2I_{-2,4}+mG_3I_{-2,5}+mG_4I_{-2,6}$$
$$+ nG_5I_{-2,3}+nG_6I_{-2,4})+\nu j^2G_6I_{-1,3}+2\nu(mG_1I_{0,1}+mG_2I_{0,2}$$
$$+ mG_3I_{0,3}+mG_4I_{0,4}+nG_5I_{0,1}+nG_6I_{0,2})+3\nu m(G_2I_{0,2}$$
$$+2G_3I_{0,3}+3G_4I_{0,4})\}$$

$$B^j_{2,4} = \pi C\{3G_6I_{1,2}+j^2(mG_1I_{-2,4}+mG_2I_{-2,5}+mG_3I_{-2,6}+mG_4I_{-2,7}$$
$$+nG_5I_{-2,4}+nG_6I_{-2,5})+\nu j^2G_6I_{-1,4}+3\nu(mG_1I_{0,2}+mG_2I_{0,3}$$
$$+mG_3I_{0,4}+mG_4I_{0,5}+nG_5I_{0,2}+nG_6I_{0,3})+4\nu m(G_2I_{0,3}$$
$$+2G_3I_{0,4}+3G_4I_{0,5})\}$$

$$B^j_{2,5} = \pi C\{\nu n(G_2I_{0,0}+2G_3I_{0,1}+3G_4I_{0,2}) + \frac{(1-\nu)}{2}j^2(G_2I_{-1,1}$$
$$+2G_3I_{-1,2}+3G_4I_{-1,3})\}$$

$$B^j_{2,6} = \pi C\{(G_2I_{1,0}+2G_3I_{1,1}+3G_4I_{1,2})+\nu n(G_2I_{0,1}+2G_3I_{0,2}$$
$$+3G_4I_{0,3}) + \frac{(1-\nu)}{2}j^2(G_2I_{-1,2}+2G_3I_{-1,3}+3G_4I_{-1,4})\}$$

$$B^j_{2,7} = \pi C\{\nu j(G_2I_{0,0}+2G_3I_{0,1}+3G_4I_{0,2}) + \frac{(1-\nu)}{2}nj(G_2I_{-1,1}$$
$$+2G_3I_{-1,2}+3G_4I_{-1,3})\}$$

$$B^j_{2,8} = \pi C\{\nu j(G_2I_{0,1}+2G_3I_{0,2}+3G_4I_{0,3}) - \frac{(1-\nu)}{2}j(G_2I_{0,1}+2G_3I_{0,2}$$
$$+3G_4I_{0,3}) + \frac{(1-\nu)}{2}nj(G_2I_{-1,2}+2G_3I_{-1,3}+3G_4I_{-1,4})\}$$

$$B^j_{3,3} = \pi C\{4G_6I_{1,2}+j^2(mG_1I_{-2,4}+mG_2I_{-2,5}+mG_3I_{-2,6}+mG_4I_{-2,7}$$
$$+nG_5I_{-2,4}+nG_6I_{-2,5})+\nu j^2G_6I_{-1,4}+4\nu(mG_1I_{0,2}+mG_2I_{0,3}$$
$$+mG_3I_{0,4}+mG_4I_{0,5}+nG_5I_{0,2}+nG_6I_{0,3})+4\nu m(G_2I_{0,3}$$
$$+2G_3I_{0,4}+3G_4I_{0,5})\}$$

$$B^j_{3,4} = \pi C\{6G_6I_{1,3}+j^2(mG_1I_{-2,5}+mG_2I_{-2,6}+mG_3I_{-2,7}+mG_4I_{-2,8}$$
$$+nG_5I_{-2,5}+nG_6I_{-2,6})+\nu j^2G_6I_{-1,5}+6\nu(mG_1I_{0,3}+mG_2I_{0,4}$$
$$+mG_3I_{0,5}+mG_4I_{0,6}+nG_5I_{0,3}+nG_6I_{0,4})+5\nu m(G_2I_{0,4}$$
$$+2G_3I_{0,5}+3G_4I_{0,6})\}$$

$$B^j_{3,5} = \pi C\{2\nu n(G_2I_{0,1}+2G_3I_{0,2}+3G_4I_{0,3}) + \frac{(1-\nu)}{2}j^2(G_2I_{-1,2}$$
$$+2G_3I_{-1,3}+3G_4I_{-1,4})\}$$

$$B^j_{3,6} = \pi C\{2(G_2I_{1,1}+2G_3I_{1,2}+3G_4I_{1,3})+2\nu n(G_2I_{0,2}+2G_3I_{0,3}$$
$$+3G_4I_{0,4}) + \frac{(1-\nu)}{2}j^2(G_2I_{-1,3}+2G_3I_{-1,4}+3G_4I_{-1,5})\}$$

$$B^j_{3,7} = \pi C\{2\nu j(G_2I_{0,1}+2G_3I_{0,2}+3G_4I_{0,3}) + \frac{(1-\nu)}{2}nj(G_2I_{-1,2}$$
$$+2G_3I_{-1,3}+3G_4I_{-1,4})\}$$

$$B^j_{3,8} = \pi C\{2\nu j(G_2I_{0,2}+2G_3I_{0,3}+3G_4I_{0,4}) - \frac{(1-\nu)}{2}j(G_2I_{0,2}$$
$$+2G_3I_{0,3}+3G_4I_{0,4}) + \frac{(1-\nu)}{2}nj(G_2I_{-1,3}+2G_3I_{-1,4}$$
$$+3G_4I_{-1,5})\}$$

$$B^j_{4,4} = \pi C\{9G_6I_{1,4}+j^2(mG_1I_{-2,6}+mG_2I_{-2,7}+mG_3I_{-2,8}+mG_4I_{-2,9}$$
$$+nG_5I_{-2,6}+nG_6I_{-2,7})+\nu j^2G_6I_{-1,6}+9\nu(mG_1I_{0,4}+mG_2I_{0,5}$$
$$+mG_3I_{0,6}+mG_4I_{0,7}+nG_5I_{0,4}+nG_6I_{0,5})+6\nu m(G_2I_{0,5}$$
$$+2G_3I_{0,6}+3G_4I_{0,7})\}$$

$$B^j_{4,5} = \pi C\{3\nu n(G_2I_{0,2}+2G_3I_{0,3}+3G_4I_{0,4}) + \frac{(1-\nu)}{2}j^2(G_2I_{-1,3}$$
$$+2G_3I_{-1,4}+3G_4I_{-1,5})\}$$

$$B^j_{4,6} = \pi C\{3(G_2I_{1,2}+2G_3I_{1,3}+3G_4I_{1,4})+3\nu n(G_2I_{0,3}+2G_3I_{0,4} +3G_4I_{0,5}) + \frac{(1-\nu)}{2}j^2(G_2I_{-1,4}+2G_3I_{-1,5}+3G_4I_{-1,6})\}$$

$$B^j_{4,7} = \pi C\{3\nu j(G_2I_{0,2}+2G_3I_{0,3}+3G_4I_{0,4}) + \frac{(1-\nu)}{2}nj(G_2I_{-1,3} +2G_3I_{-1,4}+3G_4I_{-1,5})\}$$

$$B^j_{4,8} = \pi C\{3\nu j(G_2I_{0,3}+2G_3I_{0,4}+3G_4I_{0,5}) - \frac{(1-\nu)}{2}j(G_2I_{0,3} +2G_2I_{0,4}+3G_4I_{0,5}) + \frac{(1-\nu)}{2}nj(G_2I_{-1,4}+2G_3I_{-1,5} +3G_4I_{-1,6})\}$$

$$B^j_{5,5} = 0$$

$$B^j_{5,6} = 0$$

$$B^j_{5,7} = 0$$

$$B^j_{5,8} = 0$$

$$B^j_{6,6} = 0$$

$$B^j_{6,7} = 0$$

$$B^j_{6,8} = 0$$

$$B^j_{7,7} = 0$$

$$B^j_{7,8} = 0$$

$$B^j_{8,8} = 0$$

$[C^j]$ Matrix

$$C^j_{1,1} = 0$$

$$C^j_{1,2} = 0$$

$$C^j_{1,3} = 0$$

$$C^j_{1,4} = 0$$

$$C^j_{1,5} = 0$$

$$C^j_{1,6} = 0$$

$$C^j_{1,7} = \tfrac{1}{2}\pi j I_{0,0}$$

$$C^j_{1,8} = \tfrac{1}{2}\pi j I_{0,1}$$

$$C^j_{2,2} = 0$$

$$C^j_{2,3} = 0$$

$$C^j_{2,4} = 0$$

$$C^j_{2,5} = -\tfrac{1}{2}\pi I_{1,0}$$

$$C^j_{2,6} = -\tfrac{1}{2}\pi I_{1,1}$$

$$C^j_{2,7} = \tfrac{1}{2}\pi j I_{0,1}$$

$$C^j_{2,8} = \tfrac{1}{2}\pi j I_{0,2}$$

$$C^j_{3,3} = 0$$

$$C^j_{3,4} = 0$$

$$C^j_{3,5} = -\pi I_{1,1}$$

$$C^j_{3,6} = -\pi I_{1,2}$$

$$C^j_{3,7} = \tfrac{1}{2}\pi j I_{0,2}$$

$$C^j_{3,8} = \tfrac{1}{2}\pi j I_{0,3}$$

$$C^j_{4,4} = 0$$

$$C^j_{4,5} = -\tfrac{3}{2}\pi I_{1,2}$$

$$C^j_{4,6} = -\tfrac{3}{2}\pi I_{1,3}$$

$$C^j_{4,7} = \tfrac{1}{2}\pi j I_{0,3}$$

$$C^j_{4,8} = \tfrac{1}{2}\pi j I_{0,4}$$

$$C^j_{5,5} = 0$$

$$C^j_{5,6} = 0$$

$$C^j_{5,7} = 0$$

$$C^j_{5,8} = 0$$

$$C^j_{6,6} = 0$$

$$C^j_{6,7} = 0$$

$$C^j_{6,8} = 0$$

$$C^j_{7,7} = 0$$

$$C^j_{7,8} = 0$$

$$C^j_{8,8} = 0$$

APPENDIX C

THE $[C^j]$ MATRIX AND THE ADDITIONAL PART OF THE $[A^j]$ AND $[B^j]$ MATRICES FROM SANDERS' THEORY

$[A^j]$ Matrix

$$A^j_{1,1} = \pi D \frac{(1-\nu)}{2} n^2 j^2 I_{-3,0}$$

$$A^j_{1,2} = \pi D \frac{(1-\nu)}{2} n^2 j^2 I_{-3,1}$$

$$A^j_{1,3} = \pi D \frac{(1-\nu)}{2} n^2 j^2 I_{-3,2}$$

$$A^j_{1,4} = \pi D \frac{(1-\nu)}{2} n^2 j^2 I_{-3,3}$$

$$A^j_{1,5} = \pi D \frac{(1-\nu)}{4} mn j^2 I_{-3,0}$$

$$A^j_{1,6} = \pi D \frac{(1-\nu)}{4} mn j^2 I_{-3,1}$$

$$A^j_{1,7} = \pi D \left\{ mj^3 I_{-3,0} - \frac{(1-\nu)}{4} mn^2 j I_{-3,0} \right\}$$

$$A^j_{1,8} = \pi D \left\{ mj^3 I_{-3,1} + \frac{3(1-\nu)}{4} mnj I_{-2,0} - \frac{(1-\nu)}{4} mn^2 j I_{-3,1} \right\}$$

$$A^j_{2,2} = A^j_{1,3}$$

$$A^j_{2,3} = A^j_{1,4}$$

$$A^j_{2,4} = \pi D \frac{(1+\nu)}{2} n^2 j^2 I_{-3,4}$$

$$A^j_{2,5} = A^j_{1,6}$$

$$A^j_{2,6} = \pi D \frac{(1-\nu)}{4} mnj^2 I_{3,2}$$

$$A^j_{2,7} = \pi D \{ mj^3 I_{-3,1} - mnjI_{-2,0} - \frac{(1-\nu)}{4} mn^2 jI_{-3,1} \}$$

$$A^j_{2,8} = \pi D \{ mj^3 I_{-3,2} - mnjI_{-2,1} + \frac{3}{4}(1-\nu)mnjI_{-2,1} - \frac{1}{4}(1-\nu)mn^2 jI_{-3,2} \}$$

$$A^j_{3,3} = A^j_{2,4}$$

$$A^j_{3,4} = \pi D \frac{(1-\nu)}{2} n^2 j^2 I_{-3,5}$$

$$A^j_{3,5} = A^j_{2,6}$$

$$A^j_{3,6} = \pi D \frac{(1-\nu)}{4} mnj^2 I_{-3,3}$$

$$A^j_{3,7} = \pi D \{ mj^3 I_{-3,2} - 2mnjI_{-2,1} - 2\nu mjI_{-1,0} - \frac{1}{4}(1-\nu)mn^2 jI_{-3,2} \}$$

$$A^j_{3,8} = \pi D \{ mj^3 I_{-3,3} - 2mnjI_{-2,2} - 2\nu mjI_{-1,1} + \frac{3}{4}(1-\nu)mnjI_{-2,2} - \frac{1}{4}(1-\nu)mn^2 jI_{-3,3} \}$$

$$A^j_{4,4} = \pi D \frac{(1-\nu)}{2} n^2 j^2 I_{-3,6}$$

$$A^j_{4,5} = A^j_{3,6}$$

$$A^j_{4,6} = \pi D \frac{(1-\nu)}{4} mnj^2 I_{-3,4}$$

$$A^j_{4,7} = \pi D \{ mj^3 I_{-3,3} - 3mnjI_{-2,2} - 6\nu mjI_{-1,1} - \frac{1}{4}(1-\nu)mn^2 jI_{-3,3} \}$$

$$A^j_{4,8} = \pi D \{ mj^3 I_{-3,4} - 3mnjI_{-2,3} - 6\nu mjI_{-1,2} + \frac{3}{4}(1-\nu)mnjI_{-2,3} - \frac{1}{4}(1-\nu)mn^2 jI_{-3,4} \}$$

$$A^j_{5,5} = \pi D \frac{(1-\nu)}{8} m^2 j^2 I_{-3,0}$$

$$A^j_{5,6} = \pi D \frac{(1-\nu)}{8} m^2 j^2 I_{-3,1}$$

$$A^j_{5,7} = -\pi D \frac{(1-\nu)}{8} m^2 n j I_{-3,0}$$

$$A^j_{5,8} = \pi D \left\{ \frac{3}{8}(1-\nu) m^2 j I_{-2,0} - \frac{(1-\nu)}{8} m^2 n j I_{-3,1} \right\}$$

$$A^j_{6,6} = \pi D \frac{(1-\nu)}{8} m^2 j^2 I_{-3,2}$$

$$A^j_{6,7} = -\pi D \frac{(1-\nu)}{8} m^2 n j I_{-3,1}$$

$$A^j_{6,8} = \pi D \left\{ \frac{3}{8}(1-\nu) m^2 j I_{-2,1} - \frac{(1-\nu)}{8} m^2 n j I_{-3,2} \right\}$$

$$A^j_{7,7} = \pi D \left\{ m^2 j^2 I_{-3,0} + \frac{(1-\nu)}{8} m^2 n^2 I_{-3,0} \right\}$$

$$A^j_{7,8} = \pi D \left\{ m^2 j^2 I_{-3,1} + \frac{(1-\nu)}{8} (m^2 n^2 I_{-3,1} - 3 m^2 n I_{-2,0}) \right\}$$

$$A^j_{8,8} = \pi D \left\{ m^2 j^2 I_{-3,2} + \frac{(1-\nu)}{8} (9 m^2 I_{-1,0} - 6 m^2 n I_{-2,1} + m^2 n^2 I_{-3,2}) \right\}$$

The elements of $[A^o]$ are obtained from the above elements by substituting $j = 0$ and by replacing π by 2π.

[B^j] Matrix

$$B^j_{1,1} = 0$$

$$B^j_{1,2} = 0$$

$$B^j_{1,3} = 0$$

$$B^j_{1,4} = 0$$

$$B^j_{1,5} = 0$$

$$B^j_{1,6} = 0$$

$$B^j_{1,7} = \pi C\{m^2 j(I_{-2,0}G_1+I_{-2,1}G_2+I_{-2,2}G_3+I_{-2,3}G_4)+mnj(I_{-2,0}G_5 + I_{-2,1}G_6)+\nu mjI_{-1,0}G_6\}$$

$$B^j_{1,8} = \pi C\{m^2 j(I_{-2,1}G_1+I_{-2,2}G_2+I_{-2,3}G_3+I_{-2,4}G_4)+mnj(I_{-2,1}G_5 + I_{-2,2}G_6)+\nu mjI_{-1,1}G_6\}$$

$$B^j_{2,2} = 0$$

$$B^j_{2,3} = 0$$

$$B^j_{2,4} = 0$$

$$B^j_{2,5} = 0$$

$$B^j_{2,6} = 0$$

$$B^j_{2,7} = B^j_{1,8}$$

$$B^j_{2,8} = \pi C\{m^2 j(I_{-2,2}G_1+I_{-2,3}G_2+I_{-2,4}G_3+I_{-2,5}G_4)+mnj(I_{-2,2}G_5 + I_{-2,3}G_6)+\nu mjI_{-1,2}G_6\}$$

$$B^j_{3,3} = 0$$

$$B^j_{3,4} = 0$$

$$B^j_{3,5} = 0$$

$$B^j_{3,6} = 0$$

$$B^j_{3,7} = B^j_{2,8}$$

$$B^j_{3,8} = \pi C\{m^2 j(I_{-2,3}G_1+I_{-2,4}G_2+I_{-2,5}G_3+I_{-2,6}G_4)+mnj(I_{-2,3}G_5 + I_{-2,4}G_6)+\nu mjI_{-1,3}G_6\}$$

$$B^j_{4,4} = 0$$

$$B^j_{4,5} = 0$$

$$B^j_{4,6} = 0$$

$$B^j_{4,7} = B^j_{3,8}$$

$$B^j_{4,8} = \pi C\{m^2 j(I_{-2,4}G_1+I_{-2,5}G_2+I_{-2,6}G_3+I_{-2,7}G_4) + mnj(I_{-2,4}G_5 + I_{-2,5}G_6)+\nu mjI_{-1,4}G_6\}$$

$$B^j_{5,5} = \pi C\{\tfrac{1}{4}G_6(1+\nu)I_{-1,0}j^2+\tfrac{1}{4}(1+\nu)mj^2(I_{-2,0}G_1+I_{-2,1}G_2+I_{-2,2}G_3 + I_{-2,3}G_4)+\tfrac{1}{4}(1+\nu)nj^2(I_{-2,0}G_5+I_{-2,1}G_6)\}$$

$$B^j_{5,6} = \pi C\{\tfrac{1}{4}G_6(1+\nu)I_{-1,1}j^2+\tfrac{1}{4}(1+\nu)mj^2(I_{-2,1}G_1+I_{-2,2}G_2+I_{-2,3}G_3 + I_{-2,4}G_4)+\tfrac{1}{4}(1+\nu)nj^2(I_{-2,1}G_5+I_{-2,2}G_6)\}$$

$$B^j_{5,7} = \pi C\{\tfrac{1}{4}G_6(1+\nu)I_{-1,0}jn+\tfrac{1}{4}(1+\nu)mnj(I_{-2,0}G_1+I_{-2,1}G_2+I_{-2,2}G_3 + I_{-2,3}G_4)+\tfrac{1}{4}(1+\nu)n^2j(I_{-2,0}G_5+I_{-2,1}G_6) + \frac{(1-\nu)}{2}mj(I_{-1,0}G_2+2I_{-1,1}G_3+3I_{-1,2}G_4)\}$$

$$B^j_{5,8} = \pi C\{\tfrac{1}{4}G_6(1+\nu)(jI_{0,0}+jnI_{-1,1})+\tfrac{1}{4}(1+\nu)mj(I_{-1,0}G_1+I_{-1,1}G_2$$
$$+I_{-1,2}G_3+I_{-1,3}G_4)+\tfrac{1}{4}(1+\nu)nj(I_{-1,0}G_5+I_{-1,1}G_6)$$
$$+\tfrac{1}{4}(1+\nu)mnj(I_{-2,1}G_1+I_{-2,2}G_2+I_{-2,3}G_3+I_{-2,4}G_4)$$
$$+\tfrac{1}{4}(1+\nu)n^2j(I_{-2,1}G_5+I_{-2,2}G_6)+\frac{(1-\nu)}{2}mj(I_{-1,1}G_2$$
$$+2I_{-1,2}G_3+3I_{-1,3}G_4)\}$$

$$B^j_{6,6} = \pi C\{\tfrac{1}{4}G_6(1+\nu)I_{-1,2}j^2+(1+\nu)mj^2(I_{-2,2}G_1+I_{-2,3}G_2+I_{-2,4}G_3$$
$$+I_{-2,5}G_4)+\tfrac{1}{4}(1+\nu)nj^2(I_{-2,2}G_5+I_{-2,3}G_6)\}$$

$$B^j_{6,7} = \pi C\{\tfrac{1}{4}G_6(1+\nu)I_{-1,1}jn+\tfrac{1}{4}(1+\nu)mnj(I_{-2,1}G_1+I_{-2,2}G_2+I_{-2,3}G_3$$
$$+I_{-2,4}G_4)+\tfrac{1}{4}(1+\nu)n^2j(I_{-2,1}G_5+I_{-2,2}G_6)$$
$$+\frac{(1-\nu)}{2}mj(I_{-1,1}G_2+2I_{-1,2}G_3+3I_{-1,3}G_4)\}$$

$$B^j_{6,8} = \pi C\{\tfrac{1}{4}G_6(1+\nu)(jI_{0,1}+jnI_{-1,2})+\tfrac{1}{4}(1+\nu)mj(I_{-1,1}G_1+I_{-1,2}G_2$$
$$+I_{-1,3}G_3+I_{-1,4}G_4)+\tfrac{1}{4}(1+\nu)nj(I_{-1,1}G_5+I_{-1,2}G_6)$$
$$+\tfrac{1}{4}(1+\nu)mnj(I_{-2,2}G_1+I_{-2,3}G_2+I_{-2,4}G_3+I_{-2,5}G_4)$$
$$+\tfrac{1}{4}(1+\nu)n^2j(I_{-2,2}G_5+I_{-2,3}G_6)+\frac{(1-\nu)}{2}mj(I_{-1,2}G_2$$
$$+2I_{-1,3}G_3+3I_{-1,4}G_4)\}$$

$$B^j_{7,7} = \pi C\{\tfrac{1}{4}G_6(1+\nu)I_{-1,0}n^2+\tfrac{1}{4}(1+\nu)mn^2(I_{-2,0}G_1+I_{-2,1}G_2+I_{-2,2}G_3$$
$$+I_{-2,3}G_4)+\tfrac{1}{4}(1+\nu)n^3(I_{-2,0}G_5+I_{-2,1}G_6)$$
$$+(1-\nu)mn(I_{-1,0}G_2+2I_{-1,1}G_3+3I_{-1,2}G_4)+m^3(I_{-2,0}G_1$$
$$+I_{-2,1}G_2+I_{-2,2}G_3+I_{-2,3}G_4)+m^2n(I_{-2,0}G_5+I_{-2,1}G_6)$$
$$+\nu m^2I_{-1,0}G_6\}$$

$$B^j_{7,8} = \pi C\{\tfrac{1}{4}G_6(1+\nu)(nI_{0,0}+n^2I_{-1,1})+\tfrac{1}{4}(1+\nu)mn(I_{-1,0}G_1+I_{-1,1}G_2$$
$$+I_{-1,2}G_3+I_{-1,3}G_4)+m^3(I_{-2,1}G_1+I_{-2,2}G_2$$
$$+I_{-2,3}G_3+I_{-2,4}G_4)+m^2n(I_{-2,1}G_5+I_{-2,2}G_6)+\nu m^2I_{-1,1}G_6$$
$$+\tfrac{1}{4}(1+\nu)n^2(I_{-1,0}G_5+I_{-1,1}G_6)+\tfrac{1}{4}(1+\nu)mn^2(I_{-2,1}G_1$$
$$+I_{-2,2}G_2+I_{-2,3}G_3+I_{-2,4}G_4)+\tfrac{1}{4}(1+\nu)n^3(I_{-2,1}G_5$$
$$+I_{-2,2}G_6)+(1-\nu)mn(I_{-1,1}G_2+2I_{-1,2}G_3+3I_{-1,3}G_4)$$
$$-\frac{(1-\nu)}{2}m(I_{0,0}G_2+2I_{0,1}G_3+3I_{0,2}G_4)\}$$

$$B^j_{8,8} = \pi C\{\tfrac{1}{4}G_6(1+\nu)(I_{1,0}+2nI_{0,1}+n^2I_{-1,2})+\tfrac{1}{4}(1+\nu)m(I_{0,0}G_1$$
$$+I_{0,1}G_2+I_{0,2}G_3+I_{0,3}G_4)+\tfrac{1}{4}(1+\nu)n(I_{0,0}G_5+I_{0,1}G_6)$$
$$+\tfrac{1}{2}(1+\nu)mn(I_{-1,1}G_1+I_{-1,2}G_2+I_{-1,3}G_3+I_{-1,4}G_4)$$
$$+\tfrac{1}{2}(1+\nu)n^2(I_{-1,1}G_5+I_{-1,2}G_6)+\tfrac{1}{4}(1+\nu)mn^2(I_{-2,2}G_1$$
$$+I_{-2,3}G_2+I_{-2,4}G_3+I_{-2,5}G_4)+\tfrac{1}{4}(1+\nu)n^3(I_{-2,2}G_5$$
$$+I_{-2,3}G_6)+(1-\nu)mn(I_{-1,2}G_2+2I_{-1,3}G_3+3I_{-1,4}G_4)$$
$$-(1-\nu)m(I_{0,1}G_2+2I_{0,2}G_3+3I_{0,3}G_4)+m^3(I_{-2,2}G_1$$
$$+I_{-2,3}G_2+I_{-2,4}G_3+I_{-2,5}G_4)+m^2n(I_{-2,2}G_5+I_{-2,3}G_6)$$
$$+\nu m^2I_{-1,2}G_6\}$$

$[C^j]$ Matrix

$$C^j_{1,1} = \pi m I_{0,0}$$

$$C^j_{1,2} = \pi m I_{0,1}$$

$$C^j_{1,3} = \pi m I_{0,2}$$

$$C^j_{1,4} = \pi m I_{0,3}$$

$$C^j_{1,5} = \tfrac{1}{2}\pi n I_{0,0}$$

$$C^j_{1,6} = \pi\left\{\tfrac{n}{2} I_{0,1} + \tfrac{1}{2} I_{1,0}\right\}$$

$$C^j_{1,7} = \pi j I_{0,0}$$

$$C^j_{1,8} = \pi j I_{0,1}$$

$$C^j_{2,2} = C^j_{1,3}$$

$$C^j_{2,3} = C^j_{1,4}$$

$$C^j_{2,4} = \pi m I_{0,4}$$

$$C^j_{2,5} = \pi\left\{\tfrac{n}{2} I_{0,1} - \tfrac{1}{2} I_{1,0}\right\}$$

$$C^j_{2,6} = \tfrac{1}{2}\pi n I_{0,2}$$

$$C^j_{2,7} = C^j_{1,8}$$

$$C^j_{2,8} = \pi j I_{0,2}$$

$$C^j_{3,3} = C^j_{2,4}$$

$$C^j_{3,4} = \pi m I_{0,5}$$

$$C^j_{3,5} = \pi\left\{\tfrac{n}{2} I_{0,2} - I_{1,1}\right\}$$

$$C^j_{3,6} = \pi\left\{\tfrac{n}{2} I_{0,3} - \tfrac{1}{2} I_{1,2}\right\}$$

$$C^j_{3,7} = C^j_{2,8}$$

$$c^j_{3,8} = \pi j I_{0,3}$$

$$c^j_{4,4} = \pi m I_{0,6}$$

$$c^j_{4,5} = \pi\left\{\frac{n}{2} I_{0,3} - \frac{3}{2} I_{1,2}\right\}$$

$$c^j_{4,6} = \pi\left\{\frac{n}{2} I_{0,4} - I_{1,3}\right\}$$

$$c^j_{4,7} = c^j_{3,8}$$

$$c^j_{4,8} = \pi j I_{0,4}$$

$$c^j_{5,5} = 0$$

$$c^j_{5,6} = 0$$

$$c^j_{5,7} = 0$$

$$c^j_{5,8} = 0$$

$$c^j_{6,6} = 0$$

$$c^j_{6,7} = 0$$

$$c^j_{6,8} = 0$$

$$c^j_{7,7} = c^j_{1,1}$$

$$c^j_{7,8} = c^j_{1,2}$$

$$c^j_{8,8} = c^j_{1,3}$$

VITA

3

Sahus Promsit

Candidate for the Degree of

Doctor of Philosophy

Thesis: DYNAMIC STABILITY OF CONICAL SHELLS BY FINITE ELEMENTS

Major Field: Engineering (Civil)

Biographical:

Personal Data: Born at Bangkok, Thailand, March 31, 1938, the son of Kia Heung and Charoen Promsit.

Education: Attended elementary school at Bangkok, Thailand; graduated from Patoomkongkha High School, Bangkok, Thailand, in 1958; received the Bachelor of Engineering degree in Mechanical Engineering from Chulalongkorn University, Bangkok, Thailand, in March, 1963; received the Master of Science degree in Civil Engineering in May, 1965, from Oklahoma State University; completed the requirements for the Doctor of Philosophy degree in May, 1970.

Professional Experience: Graduate research assistant in the school of Civil Engineering, Oklahoma State University, 1969-1970.